Plaquette-triplon analysis of magnetic disorder and order in a trimerized spin-1 kagome Heisenberg antiferromagnet

Pratyay Ghosh, Akhilesh Kumar Verma, and Brijesh Kumar*
School of Physical Sciences, Jawaharlal Nehru University, New Delhi 110067, India
(Received 20 July 2015; published 19 January 2016)

A spin-1 Heisenberg model on trimerized kagome lattice is studied by doing a low-energy bosonic theory in terms of plaquette triplons defined on its triangular unit cells. The model considered has an intratriangle antiferromagnetic exchange interaction J (set to 1) and two intertriangle couplings $J' > 0$ (nearest neighbor) and J'' (next nearest neighbor; of both signs). The triplon analysis performed on this model investigates the stability of the trimerized singlet ground state (which is exact in the absence of intertriangle couplings) in the J'-J'' plane. It gives a quantum phase diagram that has two gapless antiferromagnetically ordered phases separated by the spin-gapped trimerized singlet phase. The trimerized singlet ground state is found to be stable on $J'' = 0$ line (the nearest-neighbor case), and on both sides of it for $J'' \neq 0$, in an extended region bounded by the critical lines of transition to the gapless antiferromagnetic phases. The gapless phase in the negative J'' region has a coplanar 120° antiferromagnetic order with $\sqrt{3} \times \sqrt{3}$ structure. In this phase, all the magnetic moments are of equal length, and the angle between any two of them on a triangle is exactly 120°. The magnetic lattice in this case has a unit cell consisting of three triangles. The other gapless phase, in the positive J'' region, is found to exhibit a different coplanar antiferromagnetic order with ordering wave vector $\mathbf{q} = (0,0)$. Here, two magnetic moments in a triangle are of the same magnitude, but shorter than the third. While the angle between two short moments is $120^\circ - 2\delta$, it is $120^\circ + \delta$ between a short and the long one. Only when $J'' = J'$, their magnitudes become equal and the relative angles 120°. The magnetic lattice in this $\mathbf{q} = (0,0)$ phase has the translational symmetry of the kagome lattice with triangular unit cells of reduced (isosceles) symmetry. This reduction in the point-group symmetry is found to show up as a difference in the intensities of certain Bragg peaks, whose ratio $I_{(1,0)}/I_{(0,1)} = 4\sin^2(\frac{\pi}{6} + \delta)$ presents an experimental measure of the deviation δ from the 120° order.

DOI: 10.1103/PhysRevB.93.014427

I. INTRODUCTION

The quantum antiferromagnets on frustrated lattices, with competing interactions, tend to disfavor magnetic ordering, and realize interesting quantum-disordered low-temperature phases (ground states) such as the quantum spin liquids, valence-bond-solid states, or the dimer or plaquette ordered singlet phases [1–4]. The kagome quantum antiferromagnet is an interesting example of a frustrated spin system, in which the frustrated geometry of the kagome lattice (a triangular lattice of the corner-sharing triangles) and the quantum fluctuations together present a serious detriment to magnetic ordering in its ground state. For instance, the low-temperature properties of $Cu_3Zn(OH)_6Cl_2$ [5,6], $BaCu_3V_2O_8(OH)_2$ [7], $[NH_4]_2[C_7H_{14}N][V_7O_6F_{18}]$ [8], and γ-$Cu_3Mg(OH)_6Cl_2$ [9], which are the realizations of the spin-$\frac{1}{2}$ kagome Heisenberg antiferromagnet (KHA), seem to indicate this. While there is a strong support for the spin-$\frac{1}{2}$ KHA with nearest-neighbor interactions to have a spin-liquid ground state, the difficult nature of this problem has made it very hard to settle the debate on the true character of its ground state [10–24]. The relatively lesser studied spin-1 and higher spin KHA's are also not very well understood.

For the spin-1 antiferromagnetic Heisenberg model on kagome lattice, which is the problem of interest to us in this paper, a nonmagnetic hexagonal-singlet-solid (HSS) ground state with gapped magnetic excitations was proposed by Hida using the exact diagonalization and cluster expansion methods [25]. A more recent study of the spin-1 KHA model using coupled-cluster method also found a nonmagnetic ground state [26]. This problem is currently in a surge of theoretical activity, motivated by the experiments on several spin-1 kagome materials [27–31]. While some of these materials do not neatly qualify as spin-1 kagome antiferromagnets (due to their ferromagnetic or glassy response), but there are some, e.g. m–MPYNN·BF_4 [27,28] and $KV_3Ge_2O_9$ [29], which clearly show frustrated antiferromagnetic behavior. While m-MPYNN·BF_4 is well known to be spin gapped at low temperatures, the behavior of $KV_3Ge_2O_9$ is reported to be more exotic. Another material, NaV_6O_{11} (a metallic vanadate), has three types of vanadium ions, of which one type forms the spin-1 kagome layers exhibiting spin-gap behavior below 243 K, accompanied by explicit trimerization [32,33]. The appearance of weak spontaneous magnetization below 65 K (due to other vanadium ions), however, undermines the trimerized singlet physics of its kagome layers.

The most recent numerical calculations using tensor network algorithms [34,35], exact diagonalization, and density matrix renormalization group (DMRG) [36] find a gapped spontaneously trimerized singlet ground state for the quantum spin-1 nearest-neighbor KHA model. There are others who either support the HSS state of Hida [37], or suggest a gapped resonating AKLT (Affleck-Kennedy-Lieb-Tasaki) loop ground state [38]. Despite the differences, they all point towards a spin-gapped nonmagnetic ground state for the spin-1 KHA with nearest-neighbor interaction, which is in clear contrast with the studies that predicted $\sqrt{3} \times \sqrt{3}$ antiferromagnetic order in its ground state [39,40]. The spin-1 kagome antiferromagnet with spin anisotropies and biquadratic interaction have also

*bkumar@mail.jnu.ac.in

been investigated [39,41], but the pure Heisenberg case is what concerns us presently. Beyond the nearest-neighbor case, the trimerized singlet ground state has also been discussed for a spin-1 KHA with certain specific second- and third-neighbor interactions [42].

Motivated by these recent studies on the ground state of spin-1 KHA, we investigate in this paper a Heisenberg model, described in Sec. II, on trimerized kagome lattice. Our basic idea and the strategy are as follows. Since the kagome lattice is a triangular lattice of corner-sharing triangles, we construct an effective theory of spin-1 KHA in terms of the eigenstates of its basic triangular units. This we do by deriving, in Sec. III A, a bosonic representation for the spin-1 operators of a triangular plaquette in terms of its singlet and triplet states. It is like the bond-operator representation of the spins of a dimer [43,44]. This effective theory, formulated in Sec. III B, allows us to study the stability of the trimerized singlet (TS) ground state with respect to the elementary triplon (dispersing triplet) excitations, and to find if there is any antiferromagnetic (AF) order. Unlike the spin-wave analysis, which is a small fluctuation bosonic theory for a given classical magnetic order, this plaquette-triplon theory is formulated with respect to the nonmagnetic TS state which is "quantum disordered." It can describe classical order as well as quantum disorder in the ground state.

From the triplon analysis performed in this paper, we find a stable TS ground state for the nearest-neighbor spin-1 KHA, in agreement with recent numerical studies [34–36]. We also find this gapped TS phase over a range of second-neighbor interaction. Eventually, for sufficiently negative second-neighbor interaction, it undergoes a transition to the gapless phase with coplanar 120°-AF order with $\sqrt{3}\times\sqrt{3}$ structure, in which the neighboring magnetic moments lie at 120° angle relative to each other, and the magnetic unit cell consists of three triangles. This AF order has been known to occur in the KHA model for large spins with second- and third-neighbor interactions [40,45]. But here, we find it for spin-1, emerging spontaneously from the quantum disordered TS state. For positive second-neighbor interaction, we find a different coplanar AF order with ordering wave vector $\mathbf{q} = (0,0)$. In this phase, the magnetic moments in a triangular unit cell are of unequal magnitudes (two short and one long), and at a deviation of δ from the 120° orientation (with $120^\circ - 2\delta$ angle between the short moments, and $120^\circ + \delta$ between the long and the short ones). This AF order has not been discussed before in kagome antiferromagnets, but here it emerges spontaneously. We discuss these findings in detail in Sec. IV, and conclude this work with a summary in Sec. V.

II. MODEL

In this paper, we study the following quantum spin-1 Hamiltonian on trimerized kagome lattice:

$$\hat{H} = J\sum_{\langle i,j\rangle}\vec{S}_i\cdot\vec{S}_j + J'\sum_{(i,j)}\vec{S}_i\cdot\vec{S}_j + J''\sum_{\langle\langle i,j\rangle\rangle}\vec{S}_i\cdot\vec{S}_j. \quad (1)$$

As depicted in Fig. 1, it is a problem of the coupled antiferromagnetic triangles. In this explicitly trimerized kagome problem, the exchange interaction J in the up (red) triangles is taken to be stronger than that in the down (green) triangles

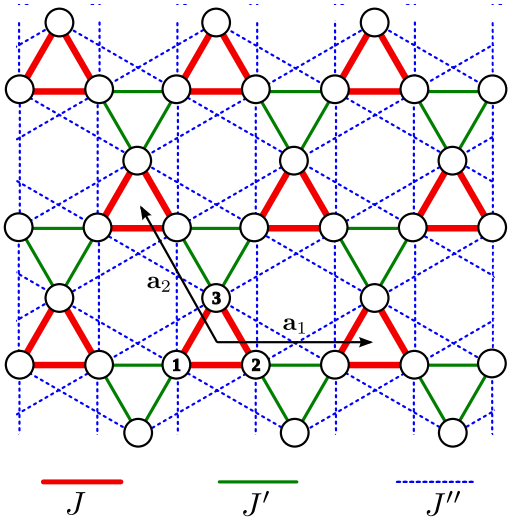

FIG. 1. The trimerized kagome lattice with intratriangle Heisenberg exchange interaction J (thick red line) and the intertriangle exchange couplings J' (green) and J'' (dashed blue line). The $\mathbf{a}_1 = 2\hat{x}$ and $\mathbf{a}_2 = -\hat{x} + \sqrt{3}\hat{y}$ are two primitive vectors of this lattice.

J'. It resembles, *for instance*, the trimerized kagome layers of one type of vanadium ions in NaV_6O_{11} [32]. This similarity is only partial, however, as the situation in NaV_6O_{11} is a bit more complex (and not to be dwelt upon here). We also include second-neighbor interaction J'' for generality. In Eq. (1), $\langle i,j\rangle$ denotes the spin pairs in the up triangles, (i,j) denotes the spin pairs in the down triangles, and the second-neighbor spin pairs are denoted as $\langle\langle i,j\rangle\rangle$. We take J and J' to be antiferromagnetic, and allow J'' to be positive as well as negative. The $\hat{H}$ becomes the standard nearest-neighbor KHA for $(J',J'') = (J,0)$.

A simple limiting case of the $\hat{H}$ of Eq. (1) corresponds to $(J',J'') = (0,0)$, for which the exact ground state is given by the direct product $\otimes\prod_{\triangle}|s\rangle$ of the singlet states $|s\rangle$ of the up triangles. It also has an energy gap J to the triplet excitations. Refer to Appendix A for the eigenstates of spin-1 Heisenberg model on a triangle. Since three spin-1's uniquely form a singlet, this *ideal* spin-gapped trimerized singlet ground state is also unique. How the nonzero J' and J'' affect this nonmagnetic TS ground state is the question that we try to answer here by studying its stability against the triplon excitations.

III. TRIPLON ANALYSIS

Just as in the case of dimerized quantum antiferromagnets, where the bond-operator formalism provides a convenient means to construct an effective low-energy theory [43,46], here we do a low-energy theory of the trimerized KHA model $\hat{H}$ in terms of the plaquette operators defined on the triangular unit cells of the kagome lattice. Towards this goal, we first derive a bosonic representation for the spin-1 operators of a triangle, and then formulate a simple but useful theory of $\hat{H}$ in terms of these plaquette operators. This theory will find for us the region of stability of the TS state, and identify the magnetic order, if any, in the J'-J'' plane.

A. Plaquette-operator representation of the spin-1 operators on a triangle

The spin-1 Heisenberg model on a triangle, that is $\hat{H}_\triangle = J(\mathbf{S}_1\cdot\mathbf{S}_2 + \mathbf{S}_2\cdot\mathbf{S}_3 + \mathbf{S}_1\cdot\mathbf{S}_3)$, has a unique singlet eigenstate $|s\rangle$ with eigenvalue $-3J$. It has three sets of triplets (that is, nine degenerate states with total spin equal to 1), $|t_{m\nu}\rangle$, given by $m = 1,0,\bar{1}$ (total S_z) and $\nu = 1,0,\bar{1}$. Here, -1 is denoted as $\bar{1}$, and the quantum number ν comes from the threefold rotational symmetry of $\hat{H}_\triangle$. The energy of these triplets is $-2J$. It also has two sets of quintets (10 states with total spin 2) and a heptet (7 eigenstates with total spin 3) with energies 0 and $3J$, respectively. The eigenvalue problem for $\hat{H}_\triangle$ is worked out in detail in Appendix A.

For $J > 0$, the singlet is the ground state of $\hat{H}_\triangle$ and the triplets form the elementary excitations with energy gap J. The quintets, that cost an energy $3J$ from the ground state, are the next higher excitations. Since they are safely above the triplets, in the simplest approximation, we ignore the quintets and the highest-energy heptets in writing a low-energy theory of the trimerized KHA model $\hat{H}$. Thus, we restrict the triangle's Hilbert space to have the singlet $|s\rangle$ and all the 9 triplets $|t_{m\nu}\rangle$ only. This reduced problem would nevertheless be sufficient to do a basic stability check of the TS ground state.

Like the bond-operator representation, that is known to be so useful to the studies of dimer phases [43,44,46], we derive here a plaquette-operator representation for the spin-1 operators on a triangular plaquette in the reduced basis $\{|s\rangle, |t_{m\nu}\rangle\}$. For this, let us first introduce the singlet and triplet plaquette operators $\hat{s}^\dagger$ and $\hat{t}^\dagger_{m\nu}$, that are defined as follows:

$$|s\rangle := \hat{s}^\dagger|\emptyset\rangle, \tag{2a}$$

$$|t_{m\nu}\rangle := \hat{t}^\dagger_{m\nu}|\emptyset\rangle. \tag{2b}$$

Here, $\hat{s}^\dagger$ are $t^\dagger_{m\nu}$ are the bosonic creation operators in a Fock space with vacuum $|\emptyset\rangle$. The projection of the infinite-dimensional Fock space onto the 10-dimensional Hilbert space spanned by $|s\rangle$ and $|t_{m\nu}\rangle$ is done by the following constraint on the number of these bosons:

$$\hat{s}^\dagger\hat{s} + \sum_{m,\nu}\hat{t}^\dagger_{m\nu}\hat{t}_{m\nu} = 1. \tag{3}$$

In terms of the singlet and triplet plaquette operators introduced above, the Hamiltonian of a triangle in the reduced basis can be written as follows:

$$\hat{H}_\triangle \approx -3J\hat{s}^\dagger\hat{s} - 2J\sum_{m,\nu}\hat{t}^\dagger_{m\nu}\hat{t}_{m\nu}. \tag{4}$$

Next, we represent the spin-1 operators of a triangle in terms of the plaquette operators. Following, they are written in an approximate form that is simple and useful. For more details, please refer to Appendix B:

$$S_{j,z} \approx \frac{\bar{s}}{\sqrt{3}}\{c_j\hat{Q}_{z\bar{1}} - s_j\hat{Q}_{z1}\}, \tag{5a}$$

$$S_{j,\alpha} \approx \frac{2\bar{s}}{\sqrt{3}}\{c_{j-1}\hat{Q}_{\alpha\bar{1}} - s_{j-1}\hat{Q}_{\alpha 1}\} \text{ for } \alpha = x,y. \tag{5b}$$

Here, $j = 1,2,3$ denote the spins of a triangle (see Fig. 1 for spin labels), and $\alpha = x$, y, and z their components. Moreover, $c_j = \cos(\frac{2\pi j}{3})$ and $s_j = \sin(\frac{2\pi j}{3})$. The "coordinate" operators $\hat{Q}_{\alpha\nu}$ for $\nu = 1,\bar{1}$ and $\alpha = x$, y, and z are defined as $\hat{Q}_{\alpha\nu} = (\hat{t}^\dagger_{\alpha\nu} + \hat{t}_{\alpha\nu})/\sqrt{2}$, where the operators $\hat{t}_{\alpha\nu}$ are given as follows:

$$\hat{t}_{z\nu} = (-i)^{\frac{1-\nu}{2}}\hat{t}_{0\nu}, \tag{6a}$$

$$\hat{t}_{x\nu} = (-i)^{\frac{1-\nu}{2}}(\hat{t}_{\bar{1}\nu} - \hat{t}_{1\nu})/\sqrt{2}, \tag{6b}$$

$$\hat{t}_{y\nu} = i^{\frac{1+\nu}{2}}(\hat{t}_{\bar{1}\nu} + \hat{t}_{1\nu})/\sqrt{2}. \tag{6c}$$

Likewise, we define the conjugate "momentum" operators $\hat{P}_{\alpha\nu} = i(\hat{t}^\dagger_{\alpha\nu} - \hat{t}_{\alpha\nu})/\sqrt{2}$, such that $[\hat{Q}_{\alpha\nu}, \hat{P}_{\alpha'\nu'}] = i\delta_{\alpha\alpha'}\delta_{\nu\nu'}$ and $\hat{P}^2_{\alpha\nu} + \hat{Q}^2_{\alpha\nu} = 2\hat{t}^\dagger_{\alpha\nu}\hat{t}_{\alpha\nu} + 1$. This canonical change of variables (from $\hat{t}$, $\hat{t}^\dagger$ to $\hat{P}$,$\hat{Q}$) is found to be convenient for further analysis. Since the $\nu = 0$ triplet operators $\hat{t}_{m0}$ do not appear in Eqs. (5), we keep them as they are.

Apart from neglecting the quintets and heptets, we have made two other simplifying approximations in writing Eqs. (5). One, we have treated the singlet operator $\hat{s}$ as *mean field* $\bar{s}$. Through $\bar{s}$, which is a measure of the singlet amplitude per triangle, we describe in mean-field approximation the TS phase on the kagome lattice. Two, we have ignored the terms bilinear in triplet operators (see Appendix B), which amounts to neglecting the interaction between triplets in the effective theory. These are two basic approximations of the mean-field triplon analysis. For a general discussion on triplon mean-field theory, please take a look at Refs. [43,44,46].

B. Plaquette-triplon mean-field theory

Now, we turn to the model $\hat{H}$ of Sec. II, and work out an effective theory for it in terms of the plaquette operators introduced in the previous subsection. We rewrite the intratriangle interactions (J terms) in $\hat{H}$ as Eq. (4), with $\hat{s}$ replaced by the uniform TS mean field $\bar{s}$. We also add to it the local constraint $\bar{s}^2 + \sum_{\alpha\nu}\hat{t}^\dagger_{\alpha\nu}\hat{t}_{\alpha\nu} = 1$, through an average Lagrange multiplier λ. The intertriangle interactions (J' and J'' terms) in $\hat{H}$ are rewritten using Eqs. (5). These steps lead to an effective bilinear problem of triplons that, after Fourier transformation, takes the following form in the momentum space:

$$\hat{H}_t = e_0 N + \sum_{\mathbf{k}}\sum_{\alpha=x,y,z}\Bigg\{\lambda\left[\hat{t}^\dagger_{\alpha 0}(\mathbf{k})\hat{t}_{\alpha 0}(\mathbf{k}) + \frac{1}{2}\right] + \frac{1}{2}\left[\lambda\hat{\mathbf{P}}^\dagger_\alpha(\mathbf{k})\hat{\mathbf{P}}_\alpha(\mathbf{k}) + \hat{\mathbf{Q}}^\dagger_\alpha(\mathbf{k})\,\mathcal{V}_{\alpha,\mathbf{k}}\,\hat{\mathbf{Q}}_\alpha(\mathbf{k})\right]\Bigg\}. \tag{7}$$

Here, N is the total number of triangular unit cells in the kagome lattice, and $e_0 = -\bar{s}^2 J + \lambda\bar{s}^2 - 2J - \frac{11}{2}\lambda$. Moreover, the operators

$$\hat{\mathbf{Q}}_\alpha(\mathbf{k}) = \begin{bmatrix}\hat{Q}_{\alpha 1}(\mathbf{k})\\ \hat{Q}_{\alpha\bar{1}}(\mathbf{k})\end{bmatrix} \quad\text{and}\quad \hat{\mathbf{P}}_\alpha(\mathbf{k}) = \begin{bmatrix}\hat{P}_{\alpha 1}(\mathbf{k})\\ \hat{P}_{\alpha\bar{1}}(\mathbf{k})\end{bmatrix}, \tag{8}$$

where $\hat{Q}_{\alpha 1}(\mathbf{k})$ and $\hat{Q}_{\alpha\bar{1}}(\mathbf{k})$ are the Fourier components of $\hat{Q}_{\alpha 1}(\mathbf{r})$ and $\hat{Q}_{\alpha\bar{1}}(\mathbf{r})$, respectively. That is, $\hat{Q}_{\alpha\nu}(\mathbf{r}) = \frac{1}{\sqrt{N}}\sum_{\mathbf{k}} e^{i\mathbf{k}\cdot\mathbf{r}}\hat{Q}_{\alpha\nu}(\mathbf{k})$ for $\nu = 1,\bar{1}$. Here, $\mathbf{r}$ denotes the position vector of the triangular units of kagome lattice (see Fig. 1), and $\mathbf{k}$ is the wave vector in the first Brillouin zone of the corresponding reciprocal lattice (see Figs. 3 and 9). Likewise, $\hat{P}_{\alpha\nu}(\mathbf{r}) = \frac{1}{\sqrt{N}}\sum_{\mathbf{k}} e^{i\mathbf{k}\cdot\mathbf{r}}\hat{P}_{\alpha\nu}(\mathbf{k})$. Since $\hat{Q}_{\alpha\nu}(\mathbf{r})$ and $\hat{P}_{\alpha\nu}(\mathbf{r})$

are Hermitian, therefore, $\hat{Q}^{\dagger}_{\alpha\nu}(\mathbf{k}) = \hat{Q}_{\alpha\nu}(-\mathbf{k})$ and $\hat{P}^{\dagger}_{\alpha\nu}(\mathbf{k}) = \hat{P}_{\alpha\nu}(-\mathbf{k})$. Moreover, $[\hat{Q}_{\alpha\nu}(\mathbf{k}), \hat{P}_{\alpha'\nu'}(\mathbf{k}')] = i\delta_{\alpha\alpha'}\delta_{\nu\nu'}\delta_{\mathbf{k}+\mathbf{k}'=0}$, while the $\hat{Q}_{\alpha\nu}(\mathbf{k})$'s commute among themselves and the same for $\hat{P}_{\alpha\nu}(\mathbf{k})$'s.

Since the $\nu = 0$ triplon modes, denoted here by $\hat{t}_{\alpha 0}(\mathbf{k}) = \frac{1}{\sqrt{N}}\sum_{\mathbf{r}} e^{-i\mathbf{k}\cdot\mathbf{r}}\hat{t}_{\alpha 0}(\mathbf{r})$, stay decoupled and local, the effective triplon model $\hat{H}_t$ is essentially a problem of two coupled "oscillators," described by $\hat{Q}_{\alpha 1}(\mathbf{k})$ and $\hat{Q}_{\alpha\bar{1}}(\mathbf{k})$ that are coupled in Eq. (7) via

$$\mathcal{V}_{\alpha,\mathbf{k}} = \begin{bmatrix} \lambda - 2\bar{s}^2\epsilon_{\alpha 1,\mathbf{k}} & \bar{s}^2\eta_{\alpha,\mathbf{k}} \\ \bar{s}^2\eta^{*}_{\alpha,\mathbf{k}} & \lambda - 2\bar{s}^2\epsilon_{\alpha\bar{1},\mathbf{k}} \end{bmatrix}. \tag{9}$$

The $\mathcal{V}_{\alpha,\mathbf{k}}$ is a Hermitian matrix, with $\eta^{*}_{\alpha,\mathbf{k}}$ as the complex conjugate of $\eta_{\alpha,\mathbf{k}}$. The $\epsilon_{\alpha\nu,\mathbf{k}}$ and $\eta_{\alpha,\mathbf{k}}$ are given as

$$\begin{aligned}\epsilon_{x\bar{1},\mathbf{k}} &= \epsilon_{y\bar{1},\mathbf{k}} \\ &= \tfrac{1}{3}\big[J'(2\cos\mathbf{k}\cdot\mathbf{a}_3 + 2\cos\mathbf{k}\cdot\mathbf{a}_1 - \cos\mathbf{k}\cdot\mathbf{a}_2) \\ &\quad + J''(4\cos\mathbf{k}\cdot\mathbf{a}_2 + \cos\mathbf{k}\cdot\mathbf{a}_3 + \cos\mathbf{k}\cdot\mathbf{a}_1)\big], \quad (10a)\\ \epsilon_{z\bar{1},\mathbf{k}} &= \tfrac{1}{12}\big[J'(2\cos\mathbf{k}\cdot\mathbf{a}_2 + 2\cos\mathbf{k}\cdot\mathbf{a}_3 - \cos\mathbf{k}\cdot\mathbf{a}_1) \\ &\quad + J''(4\cos\mathbf{k}\cdot\mathbf{a}_1 + \cos\mathbf{k}\cdot\mathbf{a}_2 + \cos\mathbf{k}\cdot\mathbf{a}_3)\big], \quad (10b)\end{aligned}$$

$$\begin{aligned}\epsilon_{x1,\mathbf{k}} &= \epsilon_{y1,\mathbf{k}} \\ &= J'\cos\mathbf{k}\cdot\mathbf{a}_2 + J''(\cos\mathbf{k}\cdot\mathbf{a}_3 + \cos\mathbf{k}\cdot\mathbf{a}_1), \quad (11a)\\ \epsilon_{z1,\mathbf{k}} &= \tfrac{1}{4}[J'\cos\mathbf{k}\cdot\mathbf{a}_1 + J''(\cos\mathbf{k}\cdot\mathbf{a}_2 + \cos\mathbf{k}\cdot\mathbf{a}_3)], \quad (11b)\end{aligned}$$

$$\begin{aligned}\eta_{x,\mathbf{k}} &= \eta_{y,\mathbf{k}} \\ &= \frac{2}{\sqrt{3}}\{J'[e^{i\mathbf{k}\cdot\mathbf{a}_3} - e^{i\mathbf{k}\cdot\mathbf{a}_1} - i\sin\mathbf{k}\cdot\mathbf{a}_2] \\ &\quad + J''[i(\sin\mathbf{k}\cdot\mathbf{a}_1 + 2\sin\mathbf{k}\cdot\mathbf{a}_2 - \sin\mathbf{k}\cdot\mathbf{a}_3) \\ &\quad + e^{i\mathbf{k}\cdot\mathbf{a}_1} - e^{i\mathbf{k}\cdot\mathbf{a}_3}]\}, \quad (12a)\\ \eta_{z,\mathbf{k}} &= \frac{1}{2\sqrt{3}}\{J'[e^{-i\mathbf{k}\cdot\mathbf{a}_2} - e^{-i\mathbf{k}\cdot\mathbf{a}_3} - i\sin\mathbf{k}\cdot\mathbf{a}_1] \\ &\quad + J''[i(2\sin\mathbf{k}\cdot\mathbf{a}_1 + \sin\mathbf{k}\cdot\mathbf{a}_2 - \sin\mathbf{k}\cdot\mathbf{a}_3) \\ &\quad - e^{-i\mathbf{k}\cdot\mathbf{a}_2} + e^{-i\mathbf{k}\cdot\mathbf{a}_3}]\}. \quad (12b)\end{aligned}$$

Here, $\mathbf{a}_1$ and $\mathbf{a}_2$ are the primitive vectors of the trimerized kagome lattice (as shown in Fig. 1), and $\mathbf{a}_3 = \mathbf{a}_1 + \mathbf{a}_2$.

The coupled oscillator problem of $\hat{H}_t$ can be diagonalized by making a unitary rotation of $\hat{Q}_{\alpha 1}(\mathbf{k})$ and $\hat{Q}_{\alpha\bar{1}}(\mathbf{k})$ to the new "coordinates" $\hat{Q}_{\alpha+}(\mathbf{k})$ and $\hat{Q}_{\alpha-}(\mathbf{k})$, given by

$$\begin{bmatrix} \hat{Q}_{\alpha+}(\mathbf{k}) \\ \hat{Q}_{\alpha-}(\mathbf{k}) \end{bmatrix} = \mathcal{U}^{\dagger}_{\alpha,\mathbf{k}} \begin{bmatrix} \hat{Q}_{\alpha 1}(\mathbf{k}) \\ \hat{Q}_{\alpha\bar{1}}(\mathbf{k}) \end{bmatrix}. \tag{13}$$

The unitary matrix $\mathcal{U}_{\alpha,\mathbf{k}}$ that diagonalizes $\hat{H}_t$ is given as

$$\mathcal{U}_{\alpha,\mathbf{k}} = \begin{bmatrix} \cos\frac{\theta_{\alpha,\mathbf{k}}}{2} & -e^{-i\phi_{\alpha,\mathbf{k}}}\sin\frac{\theta_{\alpha,\mathbf{k}}}{2} \\ e^{i\phi_{\alpha,\mathbf{k}}}\sin\frac{\theta_{\alpha,\mathbf{k}}}{2} & \cos\frac{\theta_{\alpha,\mathbf{k}}}{2} \end{bmatrix}, \tag{14}$$

where $\theta_{\alpha,\mathbf{k}} = \tan^{-1}\{|\eta_{\alpha,\mathbf{k}}|/(\epsilon_{\alpha\bar{1},\mathbf{k}} - \epsilon_{\alpha 1,\mathbf{k}})\}$, and $\eta_{\alpha,\mathbf{k}} = |\eta_{\alpha,\mathbf{k}}|e^{-i\phi_{\alpha,\mathbf{k}}}$ with $|\eta_{\alpha,-\mathbf{k}}| = |\eta_{\alpha,\mathbf{k}}|$ and $\phi_{\alpha,-\mathbf{k}} = -\phi_{\alpha,\mathbf{k}}$.

In the diagonal form, the $\hat{H}_t$ can be written as follows:

$$\begin{aligned}\hat{H}_t = e_0 N + \sum_{\mathbf{k}}\sum_{\alpha=x,y,z}\Bigg\{\lambda\left[\hat{t}^{\dagger}_{\alpha 0}(\mathbf{k})\hat{t}_{\alpha 0}(\mathbf{k}) + \frac{1}{2}\right] \\ + \sum_{\mu=\pm} E_{\alpha\mu,\mathbf{k}}\left[\hat{t}^{\dagger}_{\alpha\mu}(\mathbf{k})\hat{t}_{\alpha\mu}(\mathbf{k}) + \frac{1}{2}\right]\Bigg\}. \end{aligned}\tag{15}$$

Here, $\hat{t}_{\alpha\mu}(\mathbf{k}) = \sqrt{\frac{E_{\alpha\mu,\mathbf{k}}}{2\lambda}}\hat{Q}_{\alpha\mu}(\mathbf{k}) + i\sqrt{\frac{\lambda}{2E_{\alpha\mu,\mathbf{k}}}}\hat{P}_{\alpha\mu}(\mathbf{k})$ are the renormalized triplon operators, and

$$E_{\alpha\mu,\mathbf{k}} = \sqrt{\lambda(\lambda - 2\bar{s}^2\xi_{\alpha\mu,\mathbf{k}})} \tag{16}$$

are the triplon energy dispersions with $\xi_{\alpha\mu,\mathbf{k}} = [(\epsilon_{\alpha\bar{1},\mathbf{k}} + \epsilon_{\alpha 1,\mathbf{k}}) - \mu\sqrt{(\epsilon_{\alpha\bar{1},\mathbf{k}} - \epsilon_{\alpha 1,\mathbf{k}})^2 + |\eta_{\alpha,\mathbf{k}}|^2}]/2$. The label $\mu = \pm$ for new operators defined in Eqs. (13) is analogous to but different from the old label ν. For a stable problem of triplons with positive energy dispersions, the ground state is given by the vacuum of the triplon excitations. Thus, for the $\hat{H}_t$ of Eq. (15), we get the following ground-state energy per unit cell:

$$e_g = e_0 + \frac{3\lambda}{2} + \frac{1}{2N}\sum_{\mathbf{k}}\sum_{\alpha=x,y,z}\sum_{\mu=\pm} E_{\alpha\mu,\mathbf{k}}. \tag{17}$$

This e_g is a function of two unknown mean-field parameters λ and $\bar{s}^2$. We determine them by minimizing e_g. That is, $\partial_\lambda e_g = 0$ and $\partial_{\bar{s}^2} e_g = 0$, which gives us the following mean-field equations:

$$\bar{s}^2 = 4 - \frac{1}{2N}\sum_{\mathbf{k}}\sum_{\alpha=x,y,z}\sum_{\mu=\pm}\frac{\lambda - \bar{s}^2\xi_{\alpha\mu,\mathbf{k}}}{E_{\alpha\mu,\mathbf{k}}}, \tag{18a}$$

$$\lambda = J + \frac{\lambda}{2N}\sum_{\mathbf{k}}\sum_{\alpha=x,y,z}\sum_{\mu=\pm}\frac{\xi_{\alpha\mu,\mathbf{k}}}{E_{\alpha\mu,\mathbf{k}}}. \tag{18b}$$

The self-consistent solution of the above mean-field equations gives the physical values of λ and $\bar{s}^2$.

This formulation offers two distinct physical solutions based on whether the triplon dispersions are *gapped* or *gapless*. The $\hat{H}_t$ has nine triplon dispersions. The three $\hat{t}_{\alpha 0,\mathbf{k}}$'s have flat dispersions at λ. Then, there are six nontrivial $E_{\alpha\mu,\mathbf{k}}$. Note that $E_{x\mu,\mathbf{k}}$ is exactly same as $E_{y\mu,\mathbf{k}}$, but they are different from $E_{z\mu,\mathbf{k}}$. When the minimum of the lowest of these dispersions in the Brillouin zone is strictly greater than zero, it means there is an energy gap that protects the TS ground state against triplon excitations. We surely expect this to happen when J' and J'' are near about zero. In this "gapped" TS phase, Eqs. (18) are applicable in the given form.

However, as the intertriangle couplings grow stronger, the triplon gap may close at some point $\mathbf{q}$ in the Brillouin zone for strong enough J' or J''. That is, $E_{\alpha\mu,\mathbf{q}} = 0$, for some lower triplon branches. If it happens, then the corresponding $\mathbf{k} = \mathbf{q}$ terms in Eqs. (18) will become singular, giving rise to triplon condensation described by the condensate density n_c, a third unknown in the problem. But, now we also have a third equation, which is the condition of gaplessness, in addition to Eqs. (18) that also need to be revised for a nonzero n_c. From our calculations described in the next section, we either get $E_{\alpha\mu,\mathbf{q}} = 0$ at $\mathbf{q} = (0,0)$ for $\alpha = x,y$ and $\mu = \pm$ in a region for $J'' > 0$, or we get $E_{\alpha-,\mathbf{q}} = 0$ for $\alpha = x,y$ at $\mathbf{q} = \pi(\hat{x} + \sqrt{3}\hat{y})/3 \equiv (\frac{\pi}{3}, \frac{\pi}{\sqrt{3}})$ in another region for $J'' < 0$.

The other dispersions are found to be always gapped (see Figs. 3, 6, and 11).

The revised equations applicable to the gapless case of $\mathbf{q} = (0,0)$ can be written as follows:

$$\lambda = 2\bar{s}^2\xi_{\alpha\mu,\mathbf{q}} \text{ (same for } \alpha = x,y \text{ and } \mu = \pm) = 2\bar{s}^2(J' + 2J''), \tag{19a}$$

$$\bar{s}^2 = 4 - n_c - \frac{1}{2N}\sum_{\mathbf{k}\neq\mathbf{q}}\sum_{\alpha=x,y}\sum_{\mu=\pm}\frac{\lambda - \bar{s}^2\xi_{\alpha\mu,\mathbf{k}}}{E_{\alpha\mu,\mathbf{k}}} - \frac{1}{2N}\sum_{\mathbf{k}}\sum_{\mu=\pm}\frac{\lambda - \bar{s}^2\xi_{z\mu,\mathbf{k}}}{E_{z\mu,\mathbf{k}}}, \tag{19b}$$

$$n_c = \bar{s}^2\left(1 - \frac{J}{\lambda}\right) - \frac{\bar{s}^2}{2N}\sum_{\mathbf{k}\neq\mathbf{q}}\sum_{\alpha=x,y}\sum_{\mu=\pm}\frac{\xi_{\alpha\mu,\mathbf{k}}}{E_{\alpha\mu,\mathbf{k}}} - \frac{\bar{s}^2}{2N}\sum_{\mathbf{k}}\sum_{\mu=\pm}\frac{\xi_{z\mu,\mathbf{k}}}{E_{z\mu,\mathbf{k}}}. \tag{19c}$$

The equation for λ here follows directly from the zero gap condition $E_{\alpha\mu,\mathbf{q}} = 0$. The other two equations are derived from Eqs. (18) by defining the condensate density, n_c as the contribution of the singular terms in Eq. (18a). That is, $n_c \equiv \frac{1}{2N}\sum_{\alpha=x,y}\sum_{\mu=\pm}(\lambda - \bar{s}^2\xi_{\alpha\mu,\mathbf{q}})/E_{\alpha\mu,\mathbf{q}}$ in the present case. For the related discussion on triplon analysis, one may look at Refs. [44,46] (which similarly study the dimer problems).

Likewise, in the other gapless phase with $\mathbf{q} = (\frac{\pi}{3}, \frac{\pi}{\sqrt{3}})$, the following equations would apply:

$$\lambda = 2\bar{s}^2\xi_{\alpha-,\mathbf{q}} \text{ (same for } \alpha = x,y) = 2\bar{s}^2(J' - 4J''), \tag{20a}$$

$$\bar{s}^2 = 4 - n_c - \frac{1}{2N}\sum_{\mathbf{k}\neq\mathbf{q}}\sum_{\alpha=x,y}\frac{\lambda - \bar{s}^2\xi_{\alpha-,\mathbf{k}}}{E_{\alpha-,\mathbf{k}}} - \frac{1}{2N}\sum_{\mathbf{k}}\left[\sum_{\alpha=x,y}\frac{\lambda - \bar{s}^2\xi_{\alpha+,\mathbf{k}}}{E_{\alpha+,\mathbf{k}}} + \sum_{\mu=\pm}\frac{\lambda - \bar{s}^2\xi_{z\mu,\mathbf{k}}}{E_{z\mu,\mathbf{k}}}\right], \tag{20b}$$

$$n_c = \bar{s}^2\left(1 - \frac{J}{\lambda}\right) - \frac{\bar{s}^2}{2N}\sum_{\mathbf{k}\neq\mathbf{q}}\sum_{\alpha=x,y}\frac{\xi_{\alpha-,\mathbf{k}}}{E_{\alpha-,\mathbf{k}}} - \frac{\bar{s}^2}{2N}\sum_{\mathbf{k}}\left[\sum_{\alpha=x,y}\frac{\xi_{\alpha+,\mathbf{k}}}{E_{\alpha+,\mathbf{k}}} + \sum_{\mu=\pm}\frac{\xi_{z\mu,\mathbf{k}}}{E_{z\mu,\mathbf{k}}}\right]. \tag{20c}$$

Here, $n_c \equiv \frac{1}{2N}\sum_{\alpha=x,y}(\lambda - \bar{s}^2\xi_{\alpha-,\mathbf{q}})/E_{\alpha-,\mathbf{q}}$. Physically, a nonzero n_c and a $\mathbf{q}$ account for the AF order with ordering wave vector $\mathbf{q}$ in the ground state. Equations (22) and (23) in Sec. IV B describe the magnetic moments in terms of n_c and $\mathbf{q}$ in the two ordered phases.

IV. RESULTS AND DISCUSSION

To determine the ground-state properties of $\hat{H}$ within the triplon mean-field theory, we numerically solve the self-consistent equations derived in the previous section. In our calculations, we put $J = 1$ and take $0 \leqslant J' \leqslant 1$. We keep the second-neighbor coupling J'' small, but allow it to take both positive and negative values ($|J''| \lesssim 0.6$).

A. Gapped trimerized singlet phase

According to the theory presented in the last section, the energy gap to triplon excitations decides if the ground state is nonmagnetic (TS) or magnetically ordered. As the trivial case of independent triangles is surely gapped and nonmagnetic, a region around $(J', J'') = (0,0)$ is also expected to be so. We identify this region of gapped TS phase by following the change in the triplon gap Δ_t by gradually increasing the intertriangle couplings J' and J''. If and when the gap closes, that is Δ_t becomes zero, it marks the quantum phase transition to an AF ordered phase. In the following, we discuss this first in the nearest-neighbor interaction model for $J'' = 0$, and then in the full model including J''.

1. $J'' = 0$

In this case, J' is the only interaction variable. We calculate the triplon gap Δ_t by solving Eqs. (18) for λ and $\bar{s}^2$ for different values of J' between 0 and 1. Figure 2 presents the calculated values of λ, $\bar{s}^2$, and Δ_t as a function of J'. At $J' = 0$, it gives $\bar{s}^2 = 1$ and $\Delta_t = 1$, which is *exact* for the independent triangles. A notable feature of these data is the nonzero triplon gap in the entire range of J' between 0 and 1. Although Δ_t first decreases as J' increases from 0, but then it turns upwards and keeps growing. It is an interesting result which states that, for $J'' = 0$, the nonmagnetic TS ground state is stable against triplon excitations, and it *adiabatically* extends all the way upto $J' = 1$, starting from the exact case at $J' = 0$. This result clearly favors the recent claims of a gapped trimerized singlet ground state for the nearest-neighbor spin-1 KHA model [34–36].

To see where the gap Δ_t comes from in the Brillouin zone, we plot the dispersions in Fig. 3. Of the nine triplon dispersions given in Eq. (15), the two flat dispersions $E_{x-,\mathbf{k}} = E_{y-,\mathbf{k}} = \sqrt{\lambda(\lambda - 2\bar{s}^2J')}$ are the lowest. Hence, the triplon gap in this case is $\Delta_t = \sqrt{\lambda(\lambda - 2\bar{s}^2J')}$. Two other dispersions $E_{\alpha+,\mathbf{k}}$ (for $\alpha = x,y$) also become degenerate with the lowest ones at $\mathbf{k} = (0,0)$, the Γ point. Moreover, $E_{z-,\mathbf{k}}$ and λ (for three $\nu = 0$

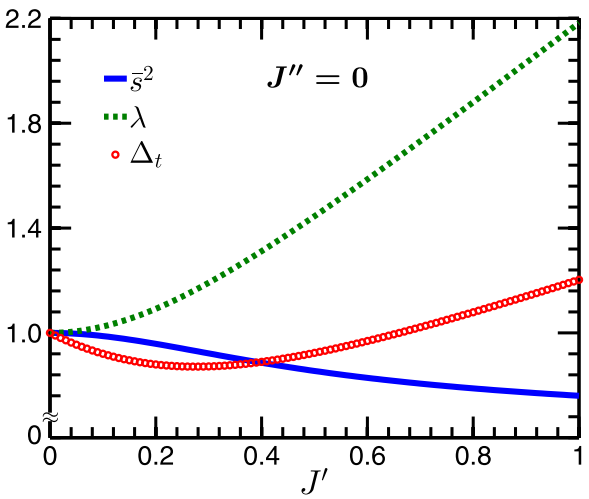

FIG. 2. The singlet weight $\bar{s}^2$, the Lagrange multiplier λ, and the triplon gap Δ_t calculated from the self-consistent Eqs. (18) for $J'' = 0$ (the nearest-neighbor case of $\hat{H}$).

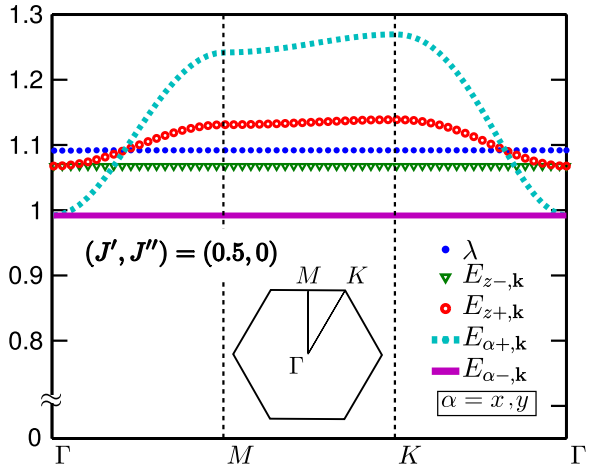

FIG. 3. The triplon dispersions [as in Eq. (15)] for the spin-1 trimerized kagome Heisenberg antiferromagnet with $J'' = 0$. Also shown here is the first Brillouin zone of this lattice.

branches) are also flat. But they are not important for the discussion here, as they are not the lowest in energy.

2. $J'' \neq 0$

While the nonmagnetic TS phase is stable for the nearest-neighbor case of $\hat{H}$, it would be nice to know how the second-neighbor interaction J'' affects it, or if it generates any magnetic order in the ground state. For the classical KHA problem, it is well known that even an infinitesimal amount of J'' causes ordering [45].

For different fixed values of J', we solve Eqs. (18) with J'' varying from 0 to ± 0.6, and follow the triplon gap. We find that a nonzero J'' makes the flat modes $E_{\alpha\mu-,\mathbf{k}}$ dispersive, which reduces the gap, and can even close it altogether. For $J'' < 0$, the triplon gap always closes at some nonzero critical value of J''. The gap also closes for $J'' > 0$, but only when $J' > 0.144$. That is, if J' is too small, then the ground state stays gapped for any positive J''. By scanning the J'-J'' plane for the critical points where the triplon gap vanishes, we compute the boundaries of the TS phase. It is found to be stable in an extended region of the J'-J'' plane. For instance, we find the TS phase for $J' = 1$ to occur in the range of $-0.245 < J'' < 0.186$, beyond which the triplon gap closes and the AF orders set in. The quantum phase diagram thus generated is shown in Fig. 4. Clearly, the case of positive J'' is more frustrated, as it favors the nonmagnetic TS phase more than the negative J''.

We identify the gapless phase for positive J'' with wave vector $\mathbf{q} = (0,0)$, the Γ point, at which the triplon gap vanishes. In the other gapless phase, for negative J'', the gap closes at the K point in Brillouin zone, that is, $\mathbf{q} = (\pi/3, \pi/\sqrt{3})$. See Figs. 6 and 11 for the dispersions in the two phases. As mentioned before, these gapless phases exhibit magnetic order through Bose condensation of triplons with their respective $\mathbf{q}$'s as the ordering wave vectors. The precise forms of the magnetic orders in the two gapless phases are described in the following.

B. Antiferromagnetically ordered phases

We now calculate the properties of the gapless phases from Eqs. (19) and (20). These equations enable the computation

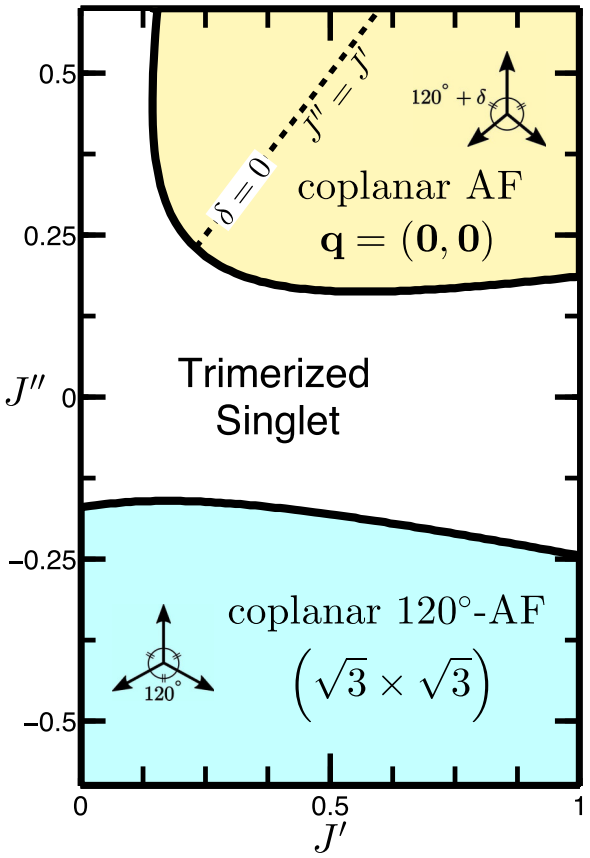

FIG. 4. The quantum phase diagram of the spin-1 trimerized kagome Heisenberg model $\hat{H}$ of Eq. (1), from triplon analysis. The gapped trimerized singlet phase, which is exact at $(J', J'') = (0,0)$, extends adiabatically up to $J' = 1$, and over a range of J''. For negative J'', it undergoes a transition to the gapless phase with coplanar 120°-antiferromagnetic order having $\sqrt{3} \times \sqrt{3}$ structure. It makes another transition, for positive J'', to a gapless coplanar antiferromagnetic phase with ordering wave vector $\mathbf{q} = (0,0)$. In this phase, the magnetic moments deviate from 120° orientations by δ, which changes with J' and J'', and becomes zero only when $J'' = J'$.

of triplon condensate density n_c in addition to giving us the quasiparticle dispersions (and $\bar{s}^2$).

The knowledge of n_c is of great physical significance. Together with $\mathbf{q}$, it determines the magnetic order in a gapless phase. A nonzero n_c implies spontaneous triplon "displacements" $\langle \hat{Q}_{\alpha\nu}(\mathbf{r}) \rangle$, which through the plaquette-operator representation given in Eqs. (5), determine the local magnetic moments $\langle \mathbf{S}_j(\mathbf{r}) \rangle$ on the kagome lattice. Since the triplons with dispersions $E_{z\mu,\mathbf{k}}$ do not condense (as they are gapped; see Figs. 6 and 11), we get $\langle \hat{Q}_{z\nu}(\mathbf{r}) \rangle = 0$. However, the condensation for $\alpha = x, y$ at $\mathbf{q}$ gives the following nonzero displacements:

$$\langle \hat{Q}_{x\bar{1}} \rangle = \sqrt{2n_{c\bar{1}}} \sin(\mathbf{q} \cdot \mathbf{r}), \quad \langle \hat{Q}_{x1} \rangle = \sqrt{2n_{c1}} \cos(\mathbf{q} \cdot \mathbf{r}), \tag{21a}$$

$$\langle \hat{Q}_{y\bar{1}} \rangle = \sqrt{2n_{c\bar{1}}} \cos(\mathbf{q} \cdot \mathbf{r}), \quad \langle \hat{Q}_{y1} \rangle = -\sqrt{2n_{c1}} \sin(\mathbf{q} \cdot \mathbf{r}). \tag{21b}$$

Here, n_{c1} and $n_{c\bar{1}}$ are the condensate densities for $\nu = 1, \bar{1}$ (that are same for $\alpha = x, y$). Hence, $n_c = 2(n_{c\bar{1}} + n_{c1})$. Since n_{c1} and $n_{c\bar{1}}$ can in general be different, we define a parameter

$\zeta = n_{c1}/n_{c\bar{1}}$. In terms of n_c and ζ, we can write $n_{c\bar{1}} = \frac{n_c}{2(1+\zeta)}$ and $n_{c1} = \frac{\zeta n_c}{2(1+\zeta)}$.

By putting these triplon displacements into the plaquette-operator representation for spins, we get the following general form of the magnetic moments:

$$\mathbf{m}_j(\mathbf{r}) = m_j(\cos[\varphi_j - \mathbf{q}\cdot\mathbf{r}], \sin[\varphi_j - \mathbf{q}\cdot\mathbf{r}], 0). \quad (22)$$

Here, $\mathbf{m}_j(\mathbf{r}) = \langle \mathbf{S}_j(\mathbf{r})\rangle$ is the magnetic moment due to jth spin in the triangular unit cell at position $\mathbf{r}$, with three components $m_{j,x}(\mathbf{r}) = m_j \cos[\varphi_j - \mathbf{q}\cdot\mathbf{r}]$, $m_{j,y}(\mathbf{r}) = m_j \sin[\varphi_j - \mathbf{q}\cdot\mathbf{r}]$, and $m_{j,z}(\mathbf{r}) = 0$. These moments are obviously *coplanar*. Their amplitudes m_j and the angles φ_j are given below for $j = 1$, 2, and 3:

$$(m_1,\varphi_1) = \left(2\bar{s}\sqrt{\frac{n_c}{3(1+\zeta)}}, \frac{\pi}{2}\right), \quad (23a)$$

$$(m_2,\varphi_2) = \left(m_1\frac{\sqrt{1+3\zeta}}{2}, \varphi_1 + \frac{2\pi}{3} + \delta\right), \quad (23b)$$

$$(m_3,\varphi_3) = \left(m_2, \varphi_1 - \frac{2\pi}{3} - \delta\right). \quad (23c)$$

Here, $\delta = \tan^{-1}[\sqrt{3}(1-\sqrt{\zeta})/(1+3\sqrt{\zeta})]$. The $\mathbf{m}_j(\mathbf{r})$'s on every triangle exactly add up to zero, as it should be in an antiferromagnetic phase. From these general considerations, now we turn to the specific cases.

1. *Coplanar AF order with* $\mathbf{q} = (0,0)$

From Eqs. (19), applicable to the phase with Goldstone mode at $\mathbf{q} = (0,0)$, we calculate λ, $\bar{s}^2$, and n_c. In Fig. 5, we plot n_c as a function of J'' for fixed values of J', alongside Δ_t of the gapped phase. It shows a quantum phase transition characterized by the triplon gap that goes to zero continuously at the critical point, and n_c that grows continuously on the other side of the critical point starting from zero at the critical point. The $\bar{s}^2$ and λ also exhibit a kinklike behavior across the transition. In Fig. 6, we show the triplon dispersions, of

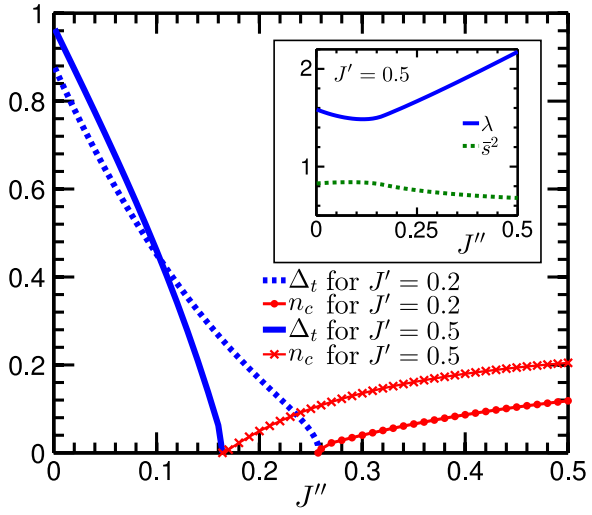

FIG. 5. The triplon gap Δ_t and the condensate density n_c vs J''. Together, they characterize the quantum phase transition from the gapped TS phase to the $\mathbf{q} = (0,0)$ AF ordered phase for $\hat{H}$ of Eq. (1). Inset: λ and $\bar{s}^2$ vs J''.

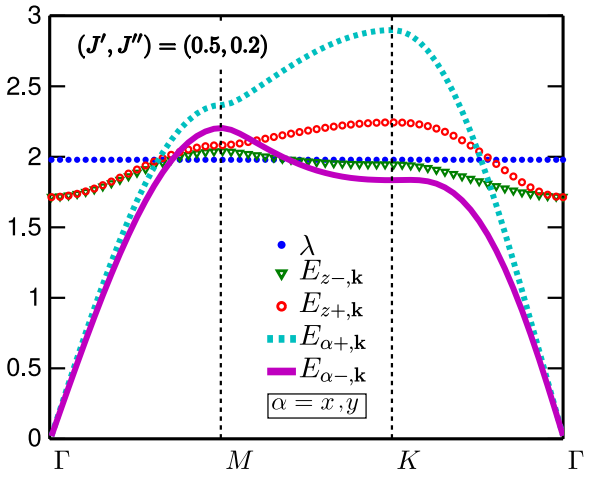

FIG. 6. The triplon dispersions [as given in Eq. (15)] in the gapless AF phase with Goldstone mode at $\mathbf{q} = (0,0)$. In this phase, the four dispersions $E_{\alpha\mu,\mathbf{k}}$ for $\alpha = x, y$ and $\mu = \pm$ go to zero linearly in $|\mathbf{k}|$, at the Γ point.

which the four dispersions with $\alpha = x, y$ and $\mu = \pm$ go to zero linearly in $|\mathbf{k}|$ at $\mathbf{q} = (0,0)$, the Γ point.

We infer the magnetic order in this phase from Eqs. (22) and (23). Its salient features are as follows. First, the magnetic moments are independent of $\mathbf{r}$, obviously because $\mathbf{q} = (0,0)$. That is, the $\mathbf{m}_j(\mathbf{r})$'s in all the triangular unit cells look identical, as shown in Fig. 7.

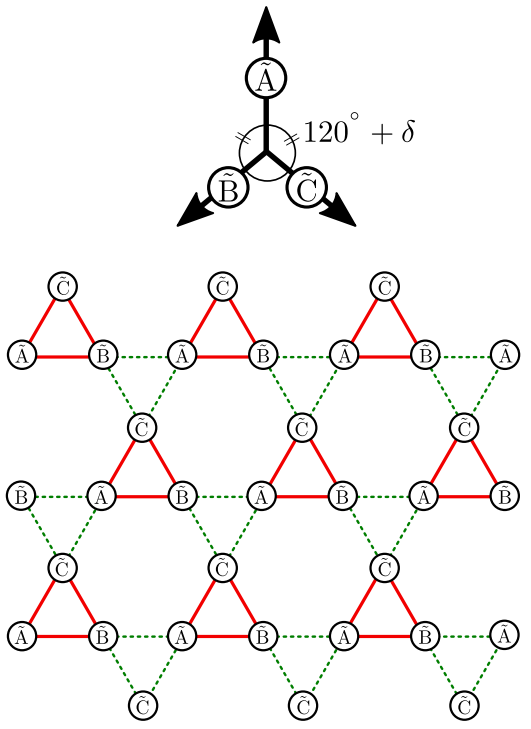

FIG. 7. The coplanar antiferromagnetic order with $\mathbf{q} = (0,0)$. Here, the magnetic moments, denoted as $\tilde{A}$, $\tilde{B}$, and $\tilde{C}$, are arranged identically in all the unit cells (red triangles). The angle between $\tilde{A}$ and $\tilde{B}$ is $120^\circ + \delta$, which is same as the angle between $\tilde{A}$ and $\tilde{C}$. The magnitude of $\tilde{B}$ is equal to that of $\tilde{C}$, but shorter than that of $\tilde{A}$. Refer to Eqs. (23) for details.

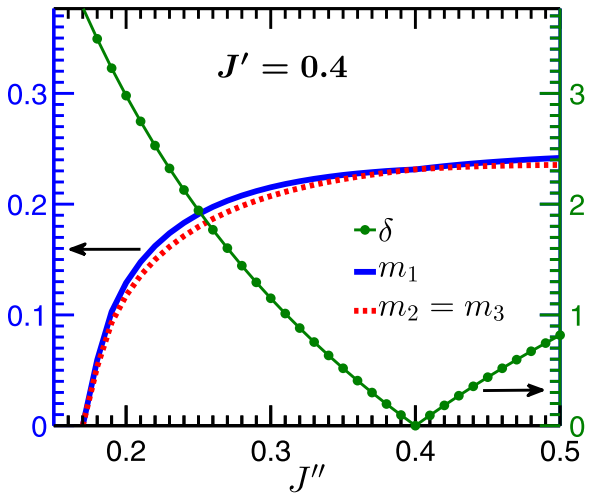

FIG. 8. The deviation δ (in degrees) from the 120° orientation and the magnitudes of the magnetic moments ($m_1 \geqslant m_2 = m_3$) in the $\mathbf{q} = (0,0)$ phase. Note that $\delta = 0$ and $m_1 = m_2 = m_3$ only when $J' = J''$.

Second, the angles between the magnetic moments in each unit cell are $\varphi_{\{2,3\}} - \varphi_1 = 120^\circ + \delta$ and $\varphi_3 - \varphi_2 = 120^\circ - 2\delta$, where δ is nonzero except when $\zeta = 1$. Their magnitudes are related as $m_1 \geqslant m_2 = m_3$, which become equal only when $\zeta = 1$. See Fig. 8 for typical values of δ and m_j's which depend upon J' and J''. These features are clearly *at variance* with the perfect 120°-AF order known from the semiclassical analysis of the KHA problem for large spins [40,45]. But then, quite unlike the semiclassical analysis, ours is a calculation with reference to the *nonmagnetic* TS state, with no presumptions of any magnetic order whatsoever. Here, the magnetic order with a deviation δ from the 120°-AF order has emerged spontaneously through the triplon dynamics present in $\hat{H}_t$. For instance, in the other gapless phase for negative J'' (to be discussed next), the same triplon analysis gives us the perfect 120°-AF order with $\sqrt{3} \times \sqrt{3}$ structure that is same as known from semiclassical analysis. Hence, the AF order that we have got here for $\mathbf{q} = (0,0)$ phase looks like a genuine finding. In fact, the semiclassical analysis would miss this order completely because there the local moments in the reference state are given to be of same magnitudes, which leave their relative-angles with no choice but to be 120° on AF triangles. In our triplon analysis, all of this is decided for itself by the triplon dynamics. We neither fix their magnitudes nor the angles from outside.

This brings us to the third point of note that is about ζ, which effects the deviation of the moments from 120° orientation through δ, and makes their magnitudes unequal. The ζ in this phase arises as the ratio of the slopes (triplon velocities) v_+ and v_- of $E_{\alpha+,\mathbf{k}}$ and $E_{\alpha-,\mathbf{k}}$ with respect to $|\mathbf{k}|$ at the Γ point. More precisely, $\zeta = \frac{v_-}{v_+} = \sqrt{\frac{J'+2J''-|J'-J''|}{J'+2J''+|J'-J''|}}$. As we see in Fig. 6, these slopes are visibly different. Therefore, in general, $\zeta < 1$ and $\delta \neq 0$. However, when $J'' = J'$, then $\zeta = 1$ and $\delta = 0^\circ$. Only in this case, the $\mathbf{q} = (0,0)$ phase has perfect 120°-AF order of the moments of equal magnitudes. In the quantum phase diagram shown in Fig. 4, this special case is highlighted by the dashed $J'' = J'$ line. On either side of this line, $\zeta < 1$ and $\delta \neq 0$. For example, close to the critical point for $J' = 1$, δ is about 9°. The typical change in δ and the magnitudes as a function of positive J'' for a fixed J' are shown in Fig. 8.

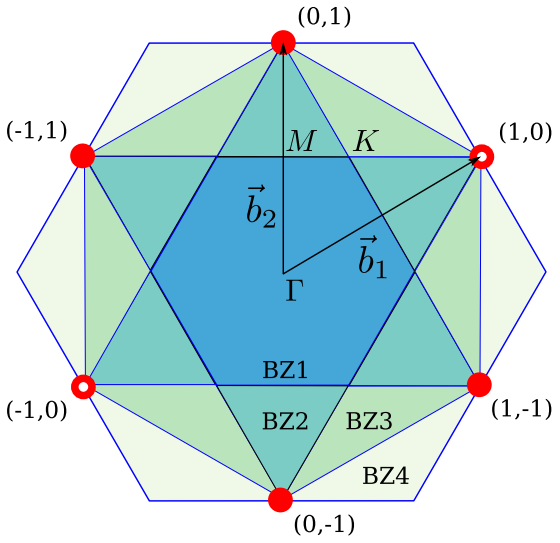

FIG. 9. The static structure factor $\mathcal{S}(\mathbf{k})$ for the coplanar magnetic order (as in Fig. 7) in the $\mathbf{q} = (0,0)$ phase. Here, $\mathbf{b}_1$ and $\mathbf{b}_2$ are the reciprocal vectors corresponding to $\mathbf{a}_1$ and $\mathbf{a}_2$ of the kagome lattice (see Fig. 1), the points on whose reciprocal lattice are given by $\mathbf{G} = \nu_1\mathbf{b}_1 + \nu_2\mathbf{b}_2$, where ν_1 and ν_2 are integers. The four filled red circles at $(\nu_1,\nu_2) = (0, \pm 1)$ and $\pm(1, -1)$ denote the Bragg peaks of equal intensity that is different from the intensity of two other equal-intensity Bragg peaks denoted as the hollow red circles at $(\pm 1,0)$. The hollow and the filled circles would all have the same intensity if $\delta = 0$. Note that the Bragg peaks occur at some corners of the higher Brillouin zones (BZ2, BZ3, BZ4), but not in the first Brillouin zone (BZ1).

Lastly, we discuss an experimental signature of this interesting $\mathbf{q} = (0,0)$ AF order on the kagome lattice. To this end, we calculate the static structure factor of the magnetic moments in this ordered state, which has the translational symmetry of the underlying kagome lattice, but has the triangular unit cells of reduced (isosceles as opposed to equilateral) rotational symmetry (due to nonzero δ). We define the static structure factor as $\mathcal{S}(\mathbf{k}) \propto |\mathbf{m}(\mathbf{k})|^2$, where $\mathbf{m}(\mathbf{k}) = \sum_{j,\mathbf{r}} e^{-i\mathbf{k}.(\mathbf{r}+\rho_j)}\mathbf{m}_j(\mathbf{r})$, with $\mathbf{r} = l_1\mathbf{a}_1 + l_2\mathbf{a}_2$ running over the Bravais lattice of the kagome lattice (l_1 and l_2 are integers) and $j = 1,2,3$. Moreover, $\rho_1 = 0$, $\rho_2 = \mathbf{a}_1/2$ and $\rho_3 = (\mathbf{a}_1 + \mathbf{a}_2)/2$ are the positions of the moments within a triangle. For the moments $\mathbf{m}_j(\mathbf{r})$, given by Eqs. (22) and (23) for $\mathbf{q} = (0,0)$, we get $\mathcal{S}(\mathbf{k}) \sim f_{\mathbf{G}}\,\delta_{\mathbf{k}=\mathbf{G}}$, where $\mathbf{G} = \nu_1\mathbf{b}_1 + \nu_2\mathbf{b}_2$ are the points of the reciprocal lattice, and the form factor $f_{\mathbf{G}}$ is given in the following:

$$f_{\mathbf{G}} = m_1^2\big[(1+3\zeta)\delta_{\nu_2=\text{odd}} + 4\delta_{\nu_1=\text{odd}}\,\delta_{\nu_2=\text{even}}\big]. \qquad (24)$$

Here, ν_1 and ν_2 are integers, and $\mathbf{b}_1 = \pi(\hat{x} + \frac{1}{\sqrt{3}}\hat{y})$ and $\mathbf{b}_2 = \frac{2\pi}{\sqrt{3}}\hat{y}$ are the primitive vectors reciprocal to the $\mathbf{a}_1$ and $\mathbf{a}_2$ of the kagome lattice (see Figs. 1 and 9).

The notable features of this $\mathcal{S}(\mathbf{k})$, that would show up in a neutron diffraction experiment, are as follows. One, the Bragg peaks do not occur when both ν_1 and ν_2 are even integers. That means, no peak at the Γ point in the first Brillouin zone (BZ1 of Fig. 9). This condition also implies that the Bragg peaks form a kagome lattice in the reciprocal space. Two, there are two

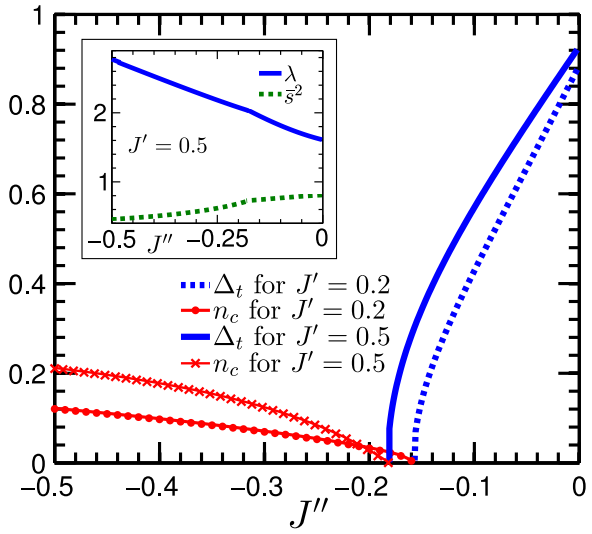

FIG. 10. The triplon gap Δ_t and the condensate density n_c describing the quantum phase transition from the gapped TS phase to the gapless phase with Goldstone mode at $\mathbf{q} = (\frac{\pi}{3}, \frac{\pi}{\sqrt{3}})$. Inset: λ and $\bar{s}^2$ vs J''.

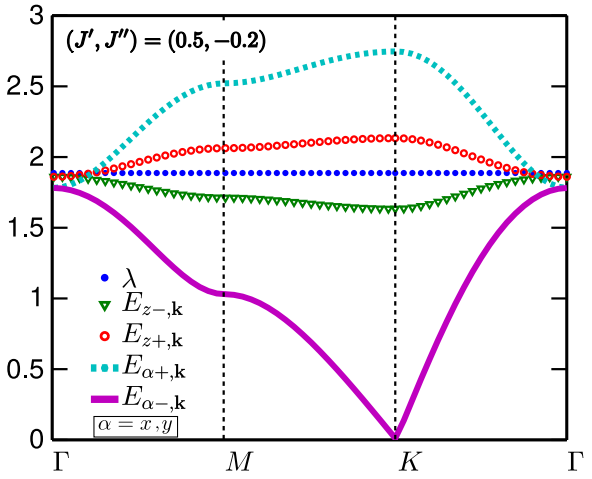

FIG. 11. The energy dispersions of the triplon excitations in the gapless AF phase with Goldstone mode at $\mathbf{q} = (\frac{\pi}{3}, \frac{\pi}{\sqrt{3}})$. Here, two degenerate dispersions $E_{x-,\mathbf{k}}$ and $E_{y-,\mathbf{k}}$ go to zero linearly at $\mathbf{q}$, that is, K point in the Brillouin zone (see Fig. 3).

sets of Bragg peaks distinguished by their intensities $I_{(\nu_1,\nu_2)}$. While the intensities of all the peaks for odd integer values of ν_2 (regardless of ν_1) are same and proportional to $(1+3\zeta)m_1^2$, for an odd ν_1 and even ν_2, the intensity is proportional to $4m_1^2$. For instance, the Bragg peaks at the four points $(\nu_1,\nu_2) = (0, \pm 1)$ and $\pm(1, -1)$ have the same intensity, which is different from the intensity of two other peaks at $(\pm 1,0)$. In Fig. 9, these two sets of Braggs peaks are shown, respectively, by the fllled and the hollow red circles. From the ratio of these intensities, one can experimentally measure ζ, and hence δ, the deviation from the 120°-AF order. One can use the formula

$$\frac{I_{(1,0)}}{I_{(0,1)}} = \frac{4}{1+3\zeta} = 4\sin^2\left(\frac{\pi}{6} + \delta\right) \tag{25}$$

to find ζ and δ. (The ζ, which is the ratio of the triplon velocities at Γ point, can also be measured alternatively by measuring triplon dispersions from inelastic neutron scattering.) Note that, for $\zeta = 1$, we get the same intensity for all the Bragg peaks, as it should be for the perfect 120°-AF order with $\mathbf{q} = (0,0)$ on the kagome lattice [47].

2. *Coplanar 120°-AF order with $\sqrt{3} \times \sqrt{3}$ structure*

The solutions of Eqs. (20) determine the nature of the gapless phase for negative J''. The condensate density n_c and other quantities, calculated as a function of J'' for fixed J', are plotted in Fig. 10. Here again, we see a continuous rise of n_c starting from zero at the critical point. Moreover, the dispersions $E_{\alpha-,\mathbf{k}}$ (for $\alpha = x, y$) go to zero linearly at $\mathbf{q} = (\pi/3, \pi/\sqrt{3}) = (\mathbf{b}_1 + \mathbf{b}_2)/3$, the K point, as shown in Fig. 11.

Interestingly, ζ is always equal to 1 in this gapless phase. This is so because the condensation of the triplons with dispersion $E_{\alpha-,\mathbf{k}}$ contributes equally to n_{c1} and $n_{c\bar{1}}$, as $\hat{Q}_{\alpha-}(\mathbf{q})$ is an equal weight linear combination of $\hat{Q}_{\alpha 1}(\mathbf{q})$ and $\hat{Q}_{\alpha\bar{1}}(\mathbf{q})$. Thus, in this phase, we have $\delta = 0$, and $m_1 = m_2 = m_3 = \bar{s}\sqrt{2n_c/3}$. That is, the magnetic moments in every triangle are equal in magnitude, and orientated at 120° angle relative to each other. But now they have $\mathbf{r}$-dependent angles $\varphi_j - \mathbf{q}\cdot\mathbf{r}$, as given in Eq. (22). It means that the magnetic moments will rotate from one triangle to another, while keeping their internal relative angles fixed at 120°.

To understand the $\mathbf{r}$ dependence of the magnetic moments, let us write $\mathbf{r}$ as $\mathbf{r} = l_1\mathbf{a}_1 + l_2\mathbf{a}_2$, where l_1 and l_2 are integers. In the present case, $\mathbf{q} = (\mathbf{b}_1 + \mathbf{b}_2)/3$, therefore, $\mathbf{q}\cdot\mathbf{r} = \frac{2\pi}{3}(l_1 + l_2)$. It immediately implies that the moments will rotate by $\frac{2\pi}{3}$, if $l_1 + l_2$ changes by -1 or 2. Or, they will rotate by $-\frac{2\pi}{3}$, if $l_1 + l_2$ changes by 1 or -2. The moments will not rotate, however, if the change in $l_1 + l_2$ occurs in integer multiples of 3. The magnetic structure that results from these considerations is shown in Fig. 12. It consists of three interpenetrating sublattices of the triangles shown in red, blue, and purple colors. The magnetic moments in the triangles of one sublattice have the same 120° orientation, which differs from the orientations on the other two sublattices by $\pm 2\pi/3$. This is the familiar coplanar 120°-AF order with $\sqrt{3} \times \sqrt{3}$ structure. In a diffraction measurement, this magnetic structure would express through the Bragg peaks at K points in the first Brillouin zone, and also at other suitable points in the extended Brillouin zone, as shown in Ref. [47].

We end this section with a brief comparative note on other studies of KHA model of quantum spins with first- and second-neighbor interactions. As it appears, there are hardly any studies on spin-1 KHA with first- and second-neighbor interactions, except for a few Schwinger boson calculations which broadly agree on the occurrence of two ordered phases [$\mathbf{q} = (0,0)$ and $\sqrt{3} \times \sqrt{3}$; both with 120°-AF order] for different signs of J'' (and $J' = J > 0$ in our notation), but undermine the quantum-disordered phase between the two for spin-1 [48,49]. They do not find any deviation from the 120°-AF order in the $\mathbf{q} = (0,0)$ phase. The studies on the corresponding spin-$\frac{1}{2}$ model, that has been investigated more actively by different methods, also claim to find the same (120°-AF) ordered phases, separated by a nonmagnetic phase [50–52]. However, in Ref. [50] for spin-$\frac{1}{2}$ J_1-J_2 KHA, the 120°-AF order for $\mathbf{q} = (0,0)$ is noted to be most

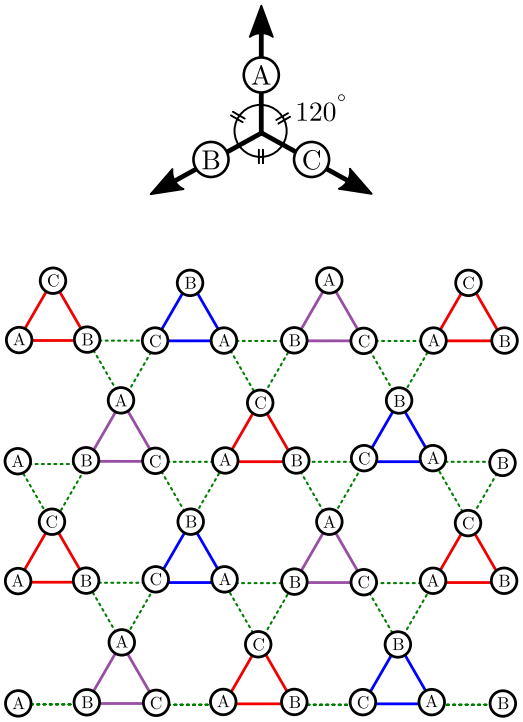

FIG. 12. The coplanar 120°-antiferromagnetic order with ordering wave vector $\mathbf{q} = (\frac{\pi}{3}, \frac{\pi}{\sqrt{3}}) = (\mathbf{b}_1 + \mathbf{b}_2)/3$. The magnetic moments, denoted as A, B, and C, in every triangle are of equal magnitude $\bar{s}\sqrt{2n_c/3}$, and form 120° angle relative to each. The moments in the triangles of same color are oriented identically, but rotated by $\pm 2\pi/3$ between the triangles of different colors. The "$\sqrt{3} \times \sqrt{3}$" magnetic lattice, formed of three interpenetrating sublattices of triangles, has a unit cell consisting of three differently colored triangles.

conspicuous when $J_2(=J'') \approx J_1(=J' = J)$, and to have enhanced numerical uncertainty away from $J_2/J_1 \approx 1$. While the first of these observations conforms to having $\delta = 0$ on $J'' = J'$ line in our Fig. 4, the second one possibly hints at the ordered phase with a nonzero δ. In the light of our Fig. 9 and Eq. (25), a careful relook at the spin structure factor of the spin-$\frac{1}{2}$ J_1-J_2 problem would be able to decide if the $\mathbf{q} = (0,0)$ phase there is of the same type as we have found here. In fact, the structure factor calculated in Ref. [52] for $J_2/J_1 = 0.4$ looks (with naked eyes) very much like our Fig. 9, with a slight difference in the intensities at (1,0) and (0,1), and the like points, suggesting a nonzero δ in the $\mathbf{q} = (0,0)$ phase.

V. SUMMARY

We now conclude by summarizing the main points. Motivated by the current research on spin-1 kagome quantum antiferromagnets, we have studied a spin-1 Heisenberg model, the $\hat{H}$ of Eq. (1), on trimerized kagome lattice (see Fig. 1). The $\hat{H}$ is a problem of coupled antiferromagnetic triangles (with intratriangle interaction $J = 1$), which in the absence of intertriangle couplings J' and J'' trivially realizes the exact TS (trimerized singlet) ground state with zero local magnetic moments and a finite-energy gap to triplet excitations. Here, we have studied the stability of this TS ground state, and its transition to ordered phases, as a function of J' and J''. This we have done by deriving a bosonic plaquette-operator representation for spin-1 operators in terms of the singlet and triplet eigenstates of a triangle [see Eqs. (5) and the Appendixes], and then writing an effective triplon model $\hat{H}_t$ of Eq. (7) for the $\hat{H}$ with reference to the TS state. The notable outcomes of this triplon analysis are as follows.

For $J'' = 0$, that is, in the nearest-neighbor case of $\hat{H}$, the TS ground state is found to be always gapped and hence stable against triplon excitations. It smoothly extends right up to $J' = 1$ (the untrimerized model), in agreement with the recent numerical findings of the same in the nearest-neighbor spin-1 kagome Heisenberg antiferromagnetic model [34–36]. The TS phase is also found to be stable over a range of J'', before undergoing transition to two gapless ordered AF (antiferromagnetic) phases, one with ordering wave vector $\mathbf{q} = (0,0)$ for positive J'', and the other with $\mathbf{q} = (\pi/3, \pi/\sqrt{3})$ for negative J''. The quantum phase diagram obtained from these calculations is presented in Fig. 4. The magnetic order in the phase with Goldstone modes at $\mathbf{q} = (\pi/3, \pi/\sqrt{3})$ is the familiar coplanar 120°-AF order with $\sqrt{3} \times \sqrt{3}$ structure (see Fig. 12). In the other AF phase with $\mathbf{q} = (0,0)$, the magnetic moments are coplanar, but of different magnitudes (two short and one long in every triangle) and deviate from 120° angle relative to each other. These deviations, characterized by an angle δ, are found to arise from the difference in the triplon velocities at $\mathbf{q} = (0,0)$ [see Figs. 6 and 7, and Eqs. (21)–(23)], and depend on J' and J''. Only when $J'' = J'$, the moments become equal in magnitude and form a perfect 120°-AF order (with $\delta = 0$). This interesting coplanar AF order with a deviation δ, for positive J'', is a new find with a scope for further investigations in the kagome antiferromagnets of low quantum spins.

ACKNOWLEDGMENTS

P.G. acknowledges CSIR (India) for financial support. B.K. acknowledges the financial support under UPE-II scheme of JNU, and DST-FIST support for the computing facility in SPS.

APPENDIX A: EIGENSTATES OF THE SPIN-1 HEISENBERG PROBLEM ON A TRIANGLE

Here, we compute the eigenstates of the Heisenberg model, given in the following, of three quantum spin-1's:

$$\hat{H}_\triangle = J(\vec{S}_1 \cdot \vec{S}_2 + \vec{S}_2 \cdot \vec{S}_3 + \vec{S}_3 \cdot \vec{S}_1). \tag{A1}$$

The $\hat{H}_\triangle$ has spin-rotation symmetry due to which the total spin $\mathbf{S} = \mathbf{S}_1 + \mathbf{S}_2 + \mathbf{S}_3$ is conserved. Therefore, its eigenstates are the total-spin eigenstates given by the total-spin quantum number $S = 0,1,2,3$, and the total-S^z with values $m = \pm 3$, ± 2, $\pm 1,0$. It also has a discrete threefold rotational symmetry that leads to an additional conserved quantum number $\nu = \pm 1,0$, describing three discrete rotations ω^ν of the triangle. Here, $\omega = e^{i2\pi/3}$ is a cube root of unity. Together, these two symmetries make it possible to exactly determine the eigenstates and eigenvalues of $\hat{H}_\triangle$.

We denote the product states of three spin-1's as $|m_1 m_2 m_3\rangle$ in the S_z basis, where $m_j = 1,0,\bar{1}$ are the eigenvalues of the spin operators $S_{j,z}$ for $j = 1,2,3$. Here, $\bar{m}$ denotes "$-m$." We use this notation for writing negative m's. First, we sectorize these states according to their total-S_z quantum number $m = m_1 + m_2 + m_3$, as given in Table I. Then, we reorganize the states within each m sector according to the

TABLE I. The basis states of $\hat{H}_\triangle$ according to their total-S_z quantum number m. The states for negative values of m can be obtained from the positive-m states by doing S_z inversion operation, that is, $1 \leftrightarrow \bar{1}$ and $0 \leftrightarrow 0$.

m	$\lvert m_1 m_2 m_3\rangle$
3	$\lvert 111\rangle$
2	$\lvert 110\rangle$, $\lvert 101\rangle$, $\lvert 011\rangle$
1	$\lvert 100\rangle$, $\lvert 010\rangle$, $\lvert 001\rangle$, $\lvert 11\bar{1}\rangle$, $\lvert 1\bar{1}1\rangle$, $\lvert \bar{1}11\rangle$
0	$\lvert 000\rangle$, $\lvert 1\bar{1}0\rangle$, $\lvert 10\bar{1}\rangle$, $\lvert 01\bar{1}\rangle$, $\lvert \bar{1}10\rangle$, $\lvert \bar{1}01\rangle$, $\lvert 0\bar{1}1\rangle$

quantum number ν of the discrete threefold rotation. The basis states in terms of m and ν are given in Table II. Since m and ν are conserved with respect to $\hat{H}_\triangle$, the states from different m-ν subspaces do not mix under $\hat{H}_\triangle$. This greatly reduces the eigenvalue problem. We finally write the $\hat{H}_\triangle$ as matrix in each m-ν subspace independently, and solve the corresponding eigenvalue problem. The eigenstates $\lvert S,m;\nu\rangle$ of $\hat{H}_\triangle$ thus found are given in the following:

Heptets. These are unique $S = 3$ and $\nu = 0$ eigenstates of $\hat{H}_\triangle$ with eigenvalue $3J$:

$$\lvert 3,3;0\rangle = \lvert 111\rangle, \tag{A2a}$$

$$\lvert 3,2;0\rangle = \frac{1}{\sqrt{3}}(\lvert 110\rangle + \lvert 101\rangle + \lvert 011\rangle), \tag{A2b}$$

$$\lvert 3,1;0\rangle = \frac{1}{\sqrt{15}}[2(\lvert 100\rangle + \lvert 010\rangle + \lvert 001\rangle) + \lvert 11\bar{1}\rangle + \lvert 1\bar{1}1\rangle + \lvert \bar{1}11\rangle], \tag{A2c}$$

$$\lvert 3,0;0\rangle = \frac{1}{\sqrt{10}}[2\lvert 000\rangle + \lvert 1\bar{1}0\rangle + \lvert \bar{1}01\rangle + \lvert 01\bar{1}\rangle + \lvert \bar{1}10\rangle + \lvert 10\bar{1}\rangle + \lvert 0\bar{1}1\rangle]. \tag{A2d}$$

TABLE II. The basis states of $\hat{H}_\triangle$ in terms of the quantum number ν of threefold rotation. To obtain negative-m states, do the S_z inversion operation on the positive-m states.

m	ν	Basis states
3	0	$\lvert 111\rangle$
	0	$\frac{1}{\sqrt{3}}(\lvert 110\rangle + \lvert 101\rangle + \lvert 011\rangle)$
2	1	$\frac{1}{\sqrt{3}}(\lvert 110\rangle + \omega\lvert 101\rangle + \omega^2\lvert 011\rangle)$
	-1	$\frac{1}{\sqrt{3}}(\lvert 110\rangle + \omega^2\lvert 101\rangle + \omega\lvert 011\rangle)$
	0	$\frac{1}{\sqrt{3}}(\lvert 100\rangle + \lvert 010\rangle + \lvert 001\rangle)$, $\frac{1}{\sqrt{3}}(\lvert 11\bar{1}\rangle + \lvert 1\bar{1}1\rangle + \lvert \bar{1}11\rangle)$
1	1	$\frac{1}{\sqrt{3}}(\lvert 100\rangle + \omega\lvert 010\rangle + \omega^2\lvert 001\rangle)$, $\frac{1}{\sqrt{3}}(\lvert 11\bar{1}\rangle + \omega\lvert 1\bar{1}1\rangle + \omega^2\lvert \bar{1}11\rangle)$
	-1	$\frac{1}{\sqrt{3}}(\lvert 100\rangle + \omega^2\lvert 010\rangle + \omega\lvert 001\rangle)$, $\frac{1}{\sqrt{3}}(\lvert 11\bar{1}\rangle + \omega^2\lvert 1\bar{1}1\rangle + \omega\lvert \bar{1}11\rangle)$
	0	$\lvert 000\rangle$, $\frac{1}{\sqrt{3}}(\lvert 10\bar{1}\rangle + \lvert 0\bar{1}1\rangle + \lvert \bar{1}10\rangle)$, $\frac{1}{\sqrt{3}}(\lvert 1\bar{1}0\rangle + \lvert \bar{1}01\rangle + \lvert 01\bar{1}\rangle)$
0	1	$\frac{1}{\sqrt{3}}(\lvert 10\bar{1}\rangle + \omega^2\lvert 0\bar{1}1\rangle + \omega\lvert \bar{1}10\rangle)$, $\frac{1}{\sqrt{3}}(\lvert 1\bar{1}0\rangle + \omega^2\lvert \bar{1}01\rangle + \omega\lvert 01\bar{1}\rangle)$
	-1	$\frac{1}{\sqrt{3}}(\lvert 10\bar{1}\rangle + \omega\lvert 0\bar{1}1\rangle + \omega^2\lvert \bar{1}10\rangle)$, $\frac{1}{\sqrt{3}}(\lvert 1\bar{1}0\rangle + \omega\lvert \bar{1}01\rangle + \omega^2\lvert 01\bar{1}\rangle)$

The negative-m eigenstates $\lvert S,\bar{m};\nu\rangle$ can be obtained by changing $\lvert m_1 m_2 m_3\rangle$ to $\lvert \bar{m}_1 \bar{m}_2 \bar{m}_3\rangle$ in the corresponding positive-m eigenstates $\lvert S,m;\nu\rangle$. For example, $\lvert 3,\bar{3}\rangle = \lvert \bar{1}\bar{1}\bar{1}\rangle$, and likewise for other negative-m eigenstates.

Quintets. These are $S = 2$ eigenstates with eigenvalue equal to 0. Here, we get two different sets of quintets, one each for $\nu = 1$ and $\bar{1}$, as written in the following:

$$\lvert 2,2;\nu\rangle = \frac{1}{\sqrt{3}}\big(\lvert 110\rangle + \omega^{\bar{\nu}}\lvert 011\rangle + \omega^{\nu}\lvert 101\rangle\big), \tag{A3a}$$

$$\lvert 2,1;\nu\rangle = \frac{1}{\sqrt{6}}\big[\lvert 100\rangle + \omega^{\nu}\lvert 010\rangle + \omega^{\bar{\nu}}\lvert 001\rangle - \big(\lvert \bar{1}11\rangle + \omega^{\nu}\lvert 1\bar{1}1\rangle + \omega^{\bar{\nu}}\lvert 11\bar{1}\rangle\big)\big], \tag{A3b}$$

$$\lvert 2,0;\nu\rangle = \frac{1}{\sqrt{6}}\big[\lvert 0\bar{1}1\rangle + \omega^{\nu}\lvert 10\bar{1}\rangle + \omega^{\bar{\nu}}\lvert \bar{1}10\rangle - \big(\lvert 1\bar{1}0\rangle + \omega^{\nu}\lvert 01\bar{1}\rangle + \omega^{\bar{\nu}}\lvert \bar{1}01\rangle\big)\big]. \tag{A3c}$$

Here, $\bar{\nu} = -\nu$, and the negative-m states can be obtained by doing the S_z inversion ($1 \leftrightarrow \bar{1}$) of the above states.

Triplets. Next, we have three sets of triplets, one each for $\nu = 0$, 1, and $\bar{1}$, with eigenvalue, $-2J$. Thus, $\hat{H}_\triangle$ has 9 degenerate $S = 1$ eigenstates. Here, we denote the triplet states $\lvert 1,m;\nu\rangle$ as $\lvert t_{m\nu}\rangle$. This slight change in notation is introduced to facilitate a convenient notation for the plaquette-operator representation (in the reduced space of the triplets and the singlet), as used in the main text (see Sec. III A). These triplets are written as follows:

(for $m = 0$ and $\nu = 0$)

$$\lvert t_{00}\rangle = \frac{1}{\sqrt{15}}\big[-3\lvert 000\rangle + \lvert 10\bar{1}\rangle + \lvert 0\bar{1}1\rangle + \lvert \bar{1}10\rangle + \lvert 1\bar{1}0\rangle + \lvert \bar{1}01\rangle + \lvert 01\bar{1}\rangle\big], \tag{A4a}$$

(for $m = 0$ and $\nu = 1,\bar{1}$)

$$\lvert t_{0\nu}\rangle = \frac{1}{\sqrt{6}}\big[\lvert 10\bar{1}\rangle + \omega^{\nu}\lvert \bar{1}10\rangle + \omega^{\bar{\nu}}\lvert 0\bar{1}1\rangle + \lvert 01\bar{1}\rangle + \omega^{\nu}\lvert \bar{1}01\rangle + \omega^{\bar{\nu}}\lvert 1\bar{1}0\rangle\big], \tag{A4b}$$

(for $m = 1,\bar{1}$ and $\nu = 0$)

$$\lvert t_{m0}\rangle = \frac{1}{\sqrt{15}}[\lvert m00\rangle + \lvert 0m0\rangle + \lvert 00m\rangle - 2(\lvert \bar{m}mm\rangle + \lvert m\bar{m}m\rangle + \lvert mm\bar{m}\rangle)], \tag{A4c}$$

(for $m = 1,\bar{1}$ and $\nu = 1,\bar{1}$)

$$\lvert t_{m\nu}\rangle = \frac{1}{\sqrt{6}}\big[\lvert m00\rangle + \omega^{\nu}\lvert 0m0\rangle + \omega^{\bar{\nu}}\lvert 00m\rangle + \lvert \bar{m}mm\rangle + \omega^{\nu}\lvert m\bar{m}m\rangle + \omega^{\bar{\nu}}\lvert mm\bar{m}\rangle\big]. \tag{A4d}$$

Singlet. Finally, we write the only singlet eigenstate, that is, $\lvert 0,0;0\rangle$, of $\hat{H}_\triangle$. It has has an eigenvalue of $-3J$. Here, we denote it as $\lvert s\rangle$:

$$\lvert s\rangle = \frac{1}{\sqrt{6}}\big[\lvert 1\bar{1}0\rangle - \lvert \bar{1}10\rangle + \lvert \bar{1}01\rangle - \lvert 10\bar{1}\rangle + \lvert 01\bar{1}\rangle - \lvert 0\bar{1}1\rangle\big]. \tag{A5}$$

For an antiferromagnetic $\hat{H}_{\triangle}$, that is $J > 0$, the singlet at $-3J$ is the lowest-energy eigenstate. The triplets at $-2J$ are the lowest excited states, while the quintets and the heptet sit further up at the higher energies.

APPENDIX B: PLAQUETTE-OPERATOR REPRESENTATION OF THE SPIN-1 OPERATORS OF A TRIANGLE

We now derive the plaquette-operator representation for the spin-1 operators of an antiferromagnetic triangle in its reduced 10-dimensional basis $\{|s\rangle, |t_{m\nu}\rangle\}$. Here, $|s\rangle$ is the singlet state and $|t_{m\nu}\rangle$'s are nine degenerate triplets given in Eqs. (A5) and (A4), respectively. This is the minimal basis that can be used to describe the low-energy dynamics of the trimerized kagome model $\hat{H}$ of Eq. (1).

The operators $S_{j,z}$ and $S_{j,+}$ are the z component and the raising operator, respectively, of the jth spin on a triangle, where $j = 1,2,3$ (see Fig. 1 for spin labels). Let us, for convenience, denote the 10 basis states as $|b_l\rangle$, where the integer l runs from 0 to 9. More precisely,

$$|b_0\rangle = |s\rangle, \tag{B1a}$$

$$|b_l\rangle = |t_{m\nu}\rangle \text{ for } l = 3m + \nu + 5, \tag{B1b}$$

where both m and $\nu = \bar{1},0,1$. In this notation, we can write the spin operators as $S_{j,z} = \sum_{l,l'} \mathcal{M}^{ll'}_{j,z} |b_l\rangle\langle b_{l'}|$ and $S_{j,+} = \sum_{l,l'} \mathcal{M}^{ll'}_{j,+} |b_l\rangle\langle b_{l'}|$, where the matrix elements are defined as $\mathcal{M}^{ll'}_{j,z} = \langle b_l|S_{j,z}|b_{l'}\rangle$ and $\mathcal{M}^{ll'}_{j,+} = \langle b_l|S_{j,+}|b_{l'}\rangle$. Next, we define the bosonic operators $\hat{b}^\dagger_l$ such that

$$|b_l\rangle := \hat{b}^\dagger_l |\emptyset\rangle. \tag{B2}$$

These plaquette operators (corresponding to the eigenstates of a triangular plaquette) live in a Fock space with vacuum $|\emptyset\rangle$ and satisfy the constraint $\sum_l \hat{b}^\dagger_l \hat{b}_l = 1$. We finally write the plaquette-operator representation of the spin-1 operators on a triangle as

$$S_{j,z} = \sum_{l,l'} \mathcal{M}^{ll'}_{j,z}\, \hat{b}^\dagger_l \hat{b}_{l'} \quad \text{and} \quad S_{j,+} = \sum_{l,l'} \mathcal{M}^{ll'}_{j,+}\, \hat{b}^\dagger_l \hat{b}_{l'}, \tag{B3}$$

where the matrices $\mathcal{M}_{j,z}$ and $\mathcal{M}_{j,+}$ are given in Eqs. (B4)–(B9), with l going from 0 for the first row to 9 for the last row, and likewise for the column index l'.

The general representation in Eq. (B3) is the basis of a more simplified plaquette-operator representation in Eqs. (5) that we have used for doing triplon analysis in the main text. There, we have approximated $\hat{s}$, that is $\hat{b}_0$, by a mean-field $\bar{s}$ and kept only those triplet terms that are coupled with $\bar{s}$, neglecting the *triplet-only* terms of Eq. (B3). This latter approximation amounts to ignoring triplon-triplon interactions in the effective theory, akin to ignoring the interaction between magnons in the linear spin-wave analysis:

$$\mathcal{M}^z_1 = \begin{pmatrix}
0 & 0 & 0 & 0 & \frac{\omega-1}{6} & 0 & \frac{\omega^2-1}{6} & 0 & 0 & 0 \\
0 & -\frac{1}{3} & -\sqrt{\frac{5}{18}} & \frac{1}{6} & 0 & 0 & 0 & 0 & 0 & 0 \\
0 & -\sqrt{\frac{5}{18}} & -\frac{1}{3} & -\sqrt{\frac{5}{18}} & 0 & 0 & 0 & 0 & 0 & 0 \\
0 & \frac{1}{6} & -\sqrt{\frac{5}{18}} & -\frac{1}{3} & 0 & 0 & 0 & 0 & 0 & 0 \\
\frac{\omega^2-1}{6} & 0 & 0 & 0 & 0 & \frac{\omega^2+1}{\sqrt{10}} & \frac{\omega+1}{2} & 0 & 0 & 0 \\
0 & 0 & 0 & 0 & \frac{\omega+1}{\sqrt{10}} & 0 & \frac{\omega^2+1}{\sqrt{10}} & 0 & 0 & 0 \\
\frac{\omega-1}{6} & 0 & 0 & 0 & \frac{\omega^2+1}{2} & \frac{\omega+1}{\sqrt{10}} & 0 & 0 & 0 & 0 \\
0 & 0 & 0 & 0 & 0 & 0 & 0 & \frac{1}{3} & \sqrt{\frac{5}{18}} & -\frac{1}{6} \\
0 & 0 & 0 & 0 & 0 & 0 & 0 & \sqrt{\frac{5}{18}} & \frac{1}{3} & \sqrt{\frac{5}{18}} \\
0 & 0 & 0 & 0 & 0 & 0 & 0 & -\frac{1}{6} & \sqrt{\frac{5}{18}} & \frac{1}{3}
\end{pmatrix}, \tag{B4}$$

$$\mathcal{M}^+_1 = \begin{pmatrix}
0 & -i\sqrt{\frac{2}{3}} & 0 & i\sqrt{\frac{2}{3}} & 0 & 0 & 0 & 0 & 0 & 0 \\
0 & 0 & 0 & 0 & 0 & 0 & 0 & 0 & 0 & 0 \\
0 & 0 & 0 & 0 & 0 & 0 & 0 & 0 & 0 & 0 \\
0 & 0 & 0 & 0 & 0 & 0 & 0 & 0 & 0 & 0 \\
0 & \frac{\omega}{3\sqrt{2}} & \frac{\omega}{3\sqrt{5}} & \frac{\omega}{3\sqrt{2}} & 0 & 0 & 0 & 0 & 0 & 0 \\
0 & -\frac{\sqrt{5}}{3} & -\frac{\sqrt{2}}{3} & -\frac{\sqrt{5}}{3} & 0 & 0 & 0 & 0 & 0 & 0 \\
0 & \frac{\omega^2}{3\sqrt{2}} & \frac{\omega^2}{3\sqrt{5}} & \frac{\omega^2}{3\sqrt{2}} & 0 & 0 & 0 & 0 & 0 & 0 \\
-i\sqrt{\frac{2}{3}} & 0 & 0 & 0 & \frac{\omega^2}{3\sqrt{2}} & -\frac{\sqrt{5}}{3} & -\frac{\sqrt{2}\omega}{3} & 0 & 0 & 0 \\
0 & 0 & 0 & 0 & \frac{4\omega^2}{3\sqrt{5}} & -\frac{\sqrt{2}}{3} & \frac{4\omega}{3\sqrt{5}} & 0 & 0 & 0 \\
i\sqrt{\frac{2}{3}} & 0 & 0 & 0 & -\frac{\sqrt{2}\omega^2}{3} & -\frac{\sqrt{5}}{3} & \frac{\omega}{3\sqrt{2}} & 0 & 0 & 0
\end{pmatrix}, \tag{B5}$$

$$\mathcal{M}_{2,z}=\begin{pmatrix}
0 & 0 & 0 & 0 & \frac{1-\omega^2}{6} & 0 & \frac{1-\omega}{6} & 0 & 0 & 0\\
0 & -\frac{1}{3} & -\frac{\sqrt{5}\omega}{3\sqrt{2}} & \frac{\omega^2}{6} & 0 & 0 & 0 & 0 & 0 & 0\\
0 & -\frac{\sqrt{5}\omega^2}{3\sqrt{2}} & -\frac{1}{3} & -\frac{\sqrt{5}\omega}{3\sqrt{2}} & 0 & 0 & 0 & 0 & 0 & 0\\
0 & \frac{\omega}{6} & -\frac{\sqrt{5}\omega^2}{3\sqrt{2}} & -\frac{1}{3} & 0 & 0 & & 0 & 0 & 0\\
\frac{1-\omega}{6} & 0 & 0 & 0 & 0 & -\frac{\omega^2}{\sqrt{10}} & -\frac{\omega}{2} & 0 & 0 & 0\\
0 & 0 & 0 & 0 & -\frac{\omega}{\sqrt{10}} & 0 & -\frac{\omega^2}{\sqrt{10}} & 0 & 0 & 0\\
\frac{1-\omega^2}{6} & 0 & 0 & 0 & -\frac{\omega^2}{2} & -\frac{\omega}{\sqrt{10}} & 0 & 0 & 0 & 0\\
0 & 0 & 0 & 0 & 0 & 0 & 0 & \frac{1}{3} & \frac{\sqrt{5}\omega}{3\sqrt{2}} & -\frac{\omega^2}{6}\\
0 & 0 & 0 & 0 & 0 & 0 & 0 & \frac{\sqrt{5}\omega^2}{3\sqrt{2}} & \frac{1}{3} & \frac{\sqrt{5}\omega}{3\sqrt{2}}\\
0 & 0 & 0 & 0 & 0 & 0 & 0 & -\frac{\omega}{6} & \frac{\sqrt{5}\omega^2}{3\sqrt{2}} & \frac{1}{3}
\end{pmatrix}, \tag{B6}$$

$$\mathcal{M}_{2,+}=\begin{pmatrix}
0 & \frac{\sqrt{2}(\omega-1)}{3} & 0 & \frac{\sqrt{2}(\omega^2-1)}{3} & 0 & 0 & 0 & 0 & 0 & 0\\
0 & 0 & 0 & 0 & 0 & 0 & 0 & 0 & 0 & 0\\
0 & 0 & 0 & 0 & 0 & 0 & 0 & 0 & 0 & 0\\
0 & 0 & 0 & 0 & 0 & 0 & 0 & 0 & 0 & 0\\
0 & \frac{\omega}{3\sqrt{2}} & \frac{\omega^2}{3\sqrt{5}} & \frac{1}{3\sqrt{2}} & 0 & 0 & 0 & 0 & 0 & 0\\
0 & -\frac{\sqrt{5}\omega^2}{3} & -\frac{\sqrt{2}}{3} & -\frac{\sqrt{5}\omega}{3} & 0 & 0 & 0 & 0 & 0 & 0\\
0 & \frac{1}{3\sqrt{2}} & \frac{\omega}{3\sqrt{5}} & \frac{\omega^2}{3\sqrt{2}} & 0 & 0 & 0 & 0 & 0 & 0\\
\frac{\sqrt{2}(1-\omega^2)}{3} & 0 & 0 & 0 & \frac{\omega^2}{3\sqrt{2}} & -\frac{\sqrt{5}\omega}{3} & -\frac{\sqrt{2}}{3} & 0 & 0 & 0\\
0 & 0 & 0 & 0 & \frac{4\omega}{3\sqrt{5}} & -\frac{\sqrt{2}}{3} & \frac{4\omega^2}{3\sqrt{5}} & 0 & 0 & 0\\
\frac{\sqrt{2}(1-\omega)}{3} & 0 & 0 & 0 & -\frac{\sqrt{2}}{3} & -\frac{\sqrt{5}\omega^2}{3} & \frac{\omega}{3\sqrt{2}} & 0 & 0 & 0
\end{pmatrix}, \tag{B7}$$

$$\mathcal{M}_{3,z}=\begin{pmatrix}
0 & 0 & 0 & 0 & -\frac{i}{2\sqrt{3}} & 0 & \frac{i}{2\sqrt{3}} & 0 & 0 & 0\\
0 & -\frac{1}{3} & -\frac{\sqrt{5}\omega^2}{3\sqrt{2}} & 0 & 0 & 0 & 0 & 0 & 0 & 0\\
0 & -\frac{\sqrt{5}\omega}{3\sqrt{2}} & -\frac{1}{3} & -\frac{\sqrt{5}\omega^2}{3\sqrt{2}} & 0 & 0 & 0 & 0 & 0 & 0\\
0 & 0 & -\frac{\sqrt{5}\omega}{3\sqrt{2}} & -\frac{1}{3} & 0 & 0 & 0 & 0 & 0 & 0\\
\frac{i}{2\sqrt{3}} & 0 & 0 & 0 & 0 & -\frac{1}{\sqrt{10}} & -\frac{1}{2} & 0 & 0 & 0\\
0 & 0 & 0 & 0 & -\frac{1}{\sqrt{10}} & 0 & -\frac{1}{\sqrt{10}} & 0 & 0 & 0\\
-\frac{i}{2\sqrt{3}} & 0 & 0 & 0 & -\frac{1}{2} & -\frac{1}{\sqrt{10}} & 0 & 0 & 0 & 0\\
0 & 0 & 0 & 0 & 0 & 0 & 0 & \frac{1}{3} & \frac{\sqrt{5}\omega^2}{3\sqrt{2}} & -\frac{\omega}{6}\\
0 & 0 & 0 & 0 & 0 & 0 & 0 & \frac{\sqrt{5}\omega}{3\sqrt{2}} & \frac{1}{3} & \frac{\sqrt{5}\omega^2}{3\sqrt{2}}\\
0 & 0 & 0 & 0 & 0 & 0 & 0 & -\frac{\omega^2}{6} & \frac{\sqrt{5}\omega}{3\sqrt{2}} & \frac{1}{3}
\end{pmatrix}, \tag{B8}$$

$$\mathcal{M}_{3,+}=\begin{pmatrix}
0 & \frac{\sqrt{2}(1-\omega^2)}{3} & 0 & \frac{\sqrt{2}(1-\omega)}{3} & 0 & 0 & 0 & 0 & 0 & 0\\
0 & 0 & 0 & 0 & 0 & 0 & 0 & 0 & 0 & 0\\
0 & 0 & 0 & 0 & 0 & 0 & 0 & 0 & 0 & 0\\
0 & 0 & 0 & 0 & 0 & 0 & 0 & 0 & 0 & 0\\
0 & \frac{\omega}{3\sqrt{2}} & \frac{1}{3\sqrt{5}} & \frac{\omega^2}{3\sqrt{2}} & 0 & 0 & 0 & 0 & 0 & 0\\
0 & -\frac{\sqrt{5}\omega}{3} & -\frac{\sqrt{2}}{3} & -\frac{\sqrt{5}\omega^2}{3} & 0 & 0 & 0 & 0 & 0 & 0\\
0 & \frac{\omega}{3\sqrt{2}} & \frac{1}{3\sqrt{5}} & \frac{\omega^2}{3\sqrt{2}} & 0 & 0 & 0 & 0 & 0 & 0\\
\frac{\sqrt{2}(\omega-1)}{3} & 0 & 0 & 0 & \frac{\omega^2}{3\sqrt{2}} & -\frac{\sqrt{5}\omega^2}{3} & -\frac{\sqrt{2}\omega^2}{3} & 0 & 0 & 0\\
0 & 0 & 0 & 0 & \frac{4}{3\sqrt{5}} & -\frac{\sqrt{2}}{3} & \frac{4}{3\sqrt{5}} & 0 & 0 & 0\\
\frac{\sqrt{2}(\omega^2-1)}{3} & 0 & 0 & 0 & -\frac{\sqrt{2}\omega}{3} & -\frac{\sqrt{5}\omega}{3} & \frac{\omega}{3\sqrt{2}} & 0 & 0 & 0
\end{pmatrix}. \tag{B9}$$

[1] W. J. Caspers, *Spin Systems* (World Scientific, Singapore, 1989).
[2] I. Bose, in *Field Theories in Condensed Matter Physics*, edited by S. Rao (Hindustan Book Agency, India, 2001).
[3] G. Misguich and C. Lhuillier, in *Frustrated Spin Systems*, edited by H. T. Diep (World Scientific, Singapore, 2005).
[4] L. Balents, Nature (London) **464**, 199 (2010).
[5] A. Olariu, P. Mendels, F. Bert, F. Duc, J. C. Trombe, M. A. de Vries, and A. Harrison, Phys. Rev. Lett. **100**, 087202 (2008).
[6] P. Mendels and F. Bert, J. Phys.: Conf. Ser. **320**, 012004 (2011).
[7] Y. Okamoto, H. Yoshida, and Z. Hiroi, J. Phys. Soc. Jpn. **78**, 033701 (2009).
[8] F. H. Aidoudi, D. W. Aldous, R. J. Goff, S. M. Z., J. P. Attfield, R. E. Morris, and P. Lightfoot, Nat. Chem. **3**, 801 (2011).
[9] R. H. Colman, A. Sinclair, and A. S. Wills, Chem. Mater. **23**, 1811 (2011).
[10] C. Zeng and V. Elser, Phys. Rev. B **42**, 8436 (1990).
[11] J. B. Marston and C. Zeng, J. Appl. Phys. **69**, 5962 (1991).
[12] J. T. Chalker and J. F. G. Eastmond, Phys. Rev. B **46**, 14201 (1992).
[13] P. W. Leung and V. Elser, Phys. Rev. B **47**, 5459 (1993).
[14] V. Subrahmanyam, Phys. Rev. B **52**, 1133 (1995).
[15] P. Lecheminant, B. Bernu, C. Lhuillier, L. Pierre, and P. Sindzingre, Phys. Rev. B **56**, 2521 (1997).
[16] F. Mila, Phys. Rev. Lett. **81**, 2356 (1998).
[17] P. Sindzingre, G. Misguich, C. Lhuillier, B. Bernu, L. Pierre, C. Waldtmann, and H.-U. Everts, Phys. Rev. Lett. **84**, 2953 (2000).
[18] M. E. Zhitomirsky and H. Tsunetsugu, Phys. Rev. B **70**, 100403(R) (2004).
[19] R. R. P. Singh and D. A. Huse, Phys. Rev. B **77**, 144415 (2008).
[20] G. Evenbly and G. Vidal, Phys. Rev. Lett. **104**, 187203 (2010).
[21] K. Hwang, Y. B. Kim, J. Yu, and K. Park, Phys. Rev. B **84**, 205133 (2011).
[22] P. H. Y. Li, R. F. Bishop, C. E. Campbell, D. J. J. Farnell, O. Götze, and J. Richter, Phys. Rev. B **86**, 214403 (2012).
[23] Y. Iqbal, F. Becca, S. Sorella, and D. Poilblanc, Phys. Rev. B **87**, 060405(R) (2013).
[24] B. K. Clark, J. M. Kinder, E. Neuscamman, G. K.-L. Chan, and M. J. Lawler, Phys. Rev. Lett. **111**, 187205 (2013).
[25] K. Hida, J. Phys. Soc. Jpn. **69**, 4003 (2000).
[26] O. Götze, D. J. J. Farnell, R. F. Bishop, P. H. Y. Li, and J. Richter, Phys. Rev. B **84**, 224428 (2011).
[27] N. Wada, T. Kobayashi, H. Yano, T. Okuno, A. Yamaguchi, and K. Awaga, J. Phys. Soc. Jpn. **66**, 961 (1997).
[28] T. Matsushita, N. Hamaguchi, K. Shimizu, N. Wada, W. Fujita, K. Awaga, A. Yamaguchi, and H. Ishimoto, J. Phys. Soc. Jpn. **79**, 093701 (2010).
[29] S. Hara, H. Sato, and Y. Narumi, J. Phys. Soc. Jpn. **81**, 073707 (2012).
[30] J. N. Behera and C. N. R. Rao, J. Am. Chem. Soc. **128**, 9334 (2006).
[31] D. Papoutsakis, D. Grohol, and D. G. Nocera, J. Am. Chem. Soc. **124**, 2647 (2002).
[32] H. Kato, M. Kato, K. Yoshimura, and K. Kosuge, J. Phys. Soc. Jpn. **70**, 1404 (2001).
[33] Y. Uchida, Y. Onoda, and Y. Kanke, J. Magn. Magn. Mater. **226-230**, 446 (2001).
[34] T. Liu, W. Li, A. Weichselbaum, J. von Delft, and G. Su, Phys. Rev. B **91**, 060403(R) (2015).
[35] T. Picot and D. Poilblanc, Phys. Rev. B **91**, 064415 (2015).
[36] H. J. Changlani and A. M. Läuchli, Phys. Rev. B **91**, 100407 (2015).
[37] S. Nishimoto and M. Nakamura, Phys. Rev. B **92**, 140412 (2015).
[38] W. Li, S. Yang, M. Cheng, Z. X. Liu, and H. H. Tu, Phys. Rev. B **89**, 174411 (2014).
[39] C. Xu and J. E. Moore, Phys. Rev. B **76**, 104427 (2007).
[40] A. Chubukov, Phys. Rev. Lett. **69**, 832 (1992).
[41] K. Damle and T. Senthil, Phys. Rev. Lett. **97**, 067202 (2006).
[42] Z. Cai, S. Chen, and Y. Wang, J. Phys.: Condens. Matter **21**, 456009 (2009).
[43] S. Sachdev and R. N. Bhatt, Phys. Rev. B **41**, 9323 (1990).
[44] B. Kumar, Phys. Rev. B **82**, 054404 (2010).
[45] A. B. Harris, C. Kallin, and A. J. Berlinsky, Phys. Rev. B **45**, 2899 (1992).
[46] R. Kumar and B. Kumar, Phys. Rev. B **77**, 144413 (2008).
[47] L. Messio, C. Lhuillier, and G. Misguich, Phys. Rev. B **83**, 184401 (2011).
[48] T. Tay and O. I. Motrunich, Phys. Rev. B **84**, 020404 (2011).
[49] L. Messio, B. Bernu, and C. Lhuillier, Phys. Rev. Lett. **108**, 207204 (2012).
[50] R. Suttner, C. Platt, J. Reuther, and R. Thomale, Phys. Rev. B **89**, 020408 (2014).
[51] Y. Iqbal, D. Poilblanc, and F. Becca, Phys. Rev. B **91**, 020402 (2015).
[52] F. Kolley, S. Depenbrock, I. P. McCulloch, U. Schollwöck, and V. Alba, Phys. Rev. B **91**, 104418 (2015).